



NASA TN D-2890

FACILITY FORM 602

N65-28738

(ACCESSION NUMBER)	(THRU)
37	1
(PAGES)	(CODE)
	30
(NASA CR OR TMX OR AD NUMBER)	(CATEGORY)

GPO PRICE \$ _____

CFSTI PRICE(S) \$ 2.00

Hard copy (HC) _____

Microfiche (MF) 50

ff 653 July 65

A STUDY OF SOLAR-SYSTEM GEOMETRIC PARAMETERS FOR USE AS INTERPLANETARY NAVIGATION AIDS

by W. Thomas Blackshear and Katherine G. Johnson

Langley Research Center

Langley Station, Hampton, Va.

A STUDY OF SOLAR-SYSTEM GEOMETRIC PARAMETERS
FOR USE AS INTERPLANETARY NAVIGATION AIDS

By W. Thomas Blackshear and Katherine G. Johnson

Langley Research Center
Langley Station, Hampton, Va.

NATIONAL AERONAUTICS AND SPACE ADMINISTRATION

For sale by the Clearinghouse for Federal Scientific and Technical Information
Springfield, Virginia 22151 - Price \$2.00

A STUDY OF SOLAR-SYSTEM GEOMETRIC PARAMETERS
FOR USE AS INTERPLANETARY NAVIGATION AIDS

By W. Thomas Blackshear and Katherine G. Johnson
Langley Research Center

SUMMARY

28738

Recognizable geometrical changes in the position of celestial bodies which may be observed by a pilot on a typical mission to Mars have been examined. Equations are presented for determining apparent positions of the Sun and planets on the celestial sphere, angular diameter of the bodies, angle between various pairs of the bodies, phases, and possible eclipses and/or occultations. Typical charts are presented which would be useful in planning interplanetary navigational procedures.

Author

INTRODUCTION

Various types of onboard navigational systems have been investigated (for example, see refs. 1, 2, and 3) which require sightings and measurements of celestial bodies. The present report is designed to provide information which would not only aid the navigator during an interplanetary mission but would aid in the premission planning of the navigational procedures. Equations are developed herein for determining the following parameters along an interplanetary trajectory: apparent positions of the Sun and planets on the celestial sphere, angular diameter of the Sun and planets, angle included at the spacecraft between various pairs of celestial bodies, and phases and/or possible eclipses of the bodies. The trace of the spacecraft heading (longitude and declination of the velocity vector) is also determined.

In the present report, the aforementioned phenomena are investigated for a typical mission to Mars. Positions of the planets were obtained from reference 4. The Navigational Star Chart (ref. 5) was used for the projections of planet and vehicle positions on the celestial sphere. The planets were chosen as reference bodies because their diameters are measurable and, whereas the stars remain relatively stationary, the planets orbit among the stars in a narrow band on either side of the ecliptic.

SYMBOLS

A	angular diameter
a	constant used in derivation of equation (9)
M_1, M_2, c_1, c_2 }	variables used in derivation of equations (9) and (11)
D	distance from spacecraft to center of celestial body
d	projection of lighted visible portion of planet onto planet diameter normal to spacecraft line of sight
P	angle between normal to planet-Sun line and normal to planet-spacecraft line
\vec{R}	position vector
r	radius of planet
T	time from exit of sphere of influence of Earth, days
X, Y, Z	rectangular right-hand axis system where X-axis is in the direction of the vernal equinox and Z-axis is in the direction of the North Celestial Pole
x, y, z	position coordinates in rectangular right-hand axis system
Υ	Aries
α	angle included at planet between Sun and spacecraft
α_1, β, γ	angles used in derivation of equation (9)
δ	declination, measured positive or negative from earth equatorial plane
η	angle included at spacecraft between pairs of bodies
λ	longitude measured westward from positive X-axis
Subscript:	
h	hours

PROCEDURE

An n-body ballistic trajectory to Mars was calculated on an electronic data processing system using the method described in reference 6, in which the spacecraft was assumed to be launched on January 4, 1967. It left the sphere of influence of Earth after 66 hours, and reached the sphere of influence of Mars after about 185 days. In the present paper, two phases of the trajectory are considered: the geocentric phase, the portion of the trajectory within the sphere of influence of Earth; and the heliocentric phase, the portion from the sphere of influence of Earth (845,000 km from Earth) to the sphere of influence of Mars (400,000 km from Mars). The portion of the trajectory within the sphere of influence of Mars is not included, inasmuch as the geometric phenomena there are analogous to those within the sphere of influence of Earth.

Planet positions and vehicle headings.- Planetary coordinates in a heliocentric Earth-equatorial system, as provided in reference 4, are given at varying intervals. The second-order Lagrange interpolation procedure (see ref. 7) was applied to these coordinate values to obtain planetary positions at times for which vehicle coordinates were calculated. The positions of the vehicle and planets in this coordinate system are shown schematically in figure 1.

Coordinates of the Sun and planets in an Earth-centered, Earth-equatorial system were obtained by the linear transformation

$$\vec{R}_{ep} = \vec{R}_{sp} - \vec{R}_{se} \quad (1)$$

where

\vec{R}_{ep} position vector from center of Earth to center of planet

\vec{R}_{sp} position vector from center of Sun to center of planet

\vec{R}_{se} position vector from center of Sun to center of Earth

Longitude measured westward from the positive X-axis was obtained by using the following equations:

$$\left. \begin{aligned} \lambda &= 270^\circ + \arctan \left| \frac{x}{y} \right| && (x > 0, y > 0) \\ \lambda &= 90^\circ - \arctan \left| \frac{x}{y} \right| && (x > 0, y < 0) \\ \lambda &= 270^\circ - \arctan \left| \frac{x}{y} \right| && (x < 0, y > 0) \\ \lambda &= 90^\circ + \arctan \left| \frac{x}{y} \right| && (x < 0, y < 0) \end{aligned} \right\} (2)$$

Declination from the Earth-equatorial plane was obtained by use of the relation

$$\delta = \text{arc tan } \frac{z}{\sqrt{x^2 + y^2}} \quad (3)$$

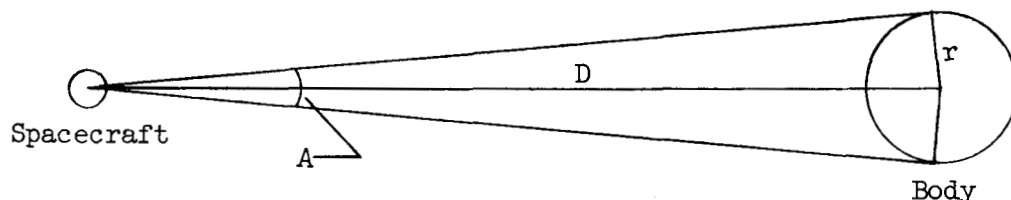
where the positive X-axis is in the direction of vernal equinox, the XY-plane contains the celestial equator, and the Z-axis is positive in the direction of the North Celestial Pole.

The spacecraft heading was determined by computing the longitude and declination of the spacecraft velocity vector (velocity with respect to the Sun) as described, using coordinates from the interplanetary trajectory program (ref. 6).

Angular diameter.- Angular diameters of Mercury, Venus, Jupiter, Saturn, Uranus, Neptune, and Pluto were obtained, under the assumption that they are spherical bodies, by the small angle approximation

$$A = \frac{2r}{D} \quad (4)$$

where D is the distance from the spacecraft to the center of the celestial body as illustrated in the following sketch:



Because of the relatively large size of the Sun and the close approaches of the spacecraft to the Earth and Mars, the angular diameters of these three bodies were obtained from the equation

$$A = 2 \text{ arc sin } \frac{r}{D} \quad (5)$$

Equation (5) is exact under the spherical-body assumption; however, it requires more computing time than equation (4). For this reason equation (4) was used whenever its application would yield sufficiently accurate results.

Included angles.- The included angles, as seen from the spacecraft, for various combinations of the solar bodies were calculated from the vector equation:

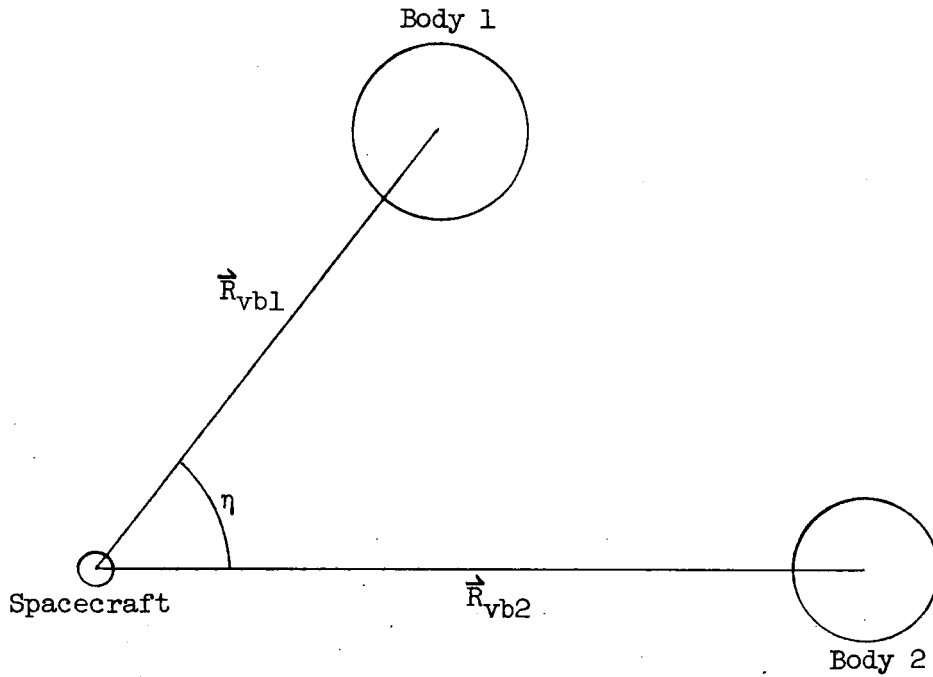
$$\eta = \text{arc cos } \frac{\vec{R}_{vb1} \cdot \vec{R}_{vb2}}{|\vec{R}_{vb1}| |\vec{R}_{vb2}|} \quad (6)$$

where

\vec{R}_{vb1} position vector from spacecraft to solar-system body 1

\vec{R}_{vb2} position vector from spacecraft to solar-system body 2

as indicated in this sketch



The position vectors from the vehicle to the bodies \vec{R}_{vbi} were obtained from the transformation

$$\vec{R}_{vbi} = \vec{R}_{ebi} - \vec{R}_{ev} \quad (7)$$

where

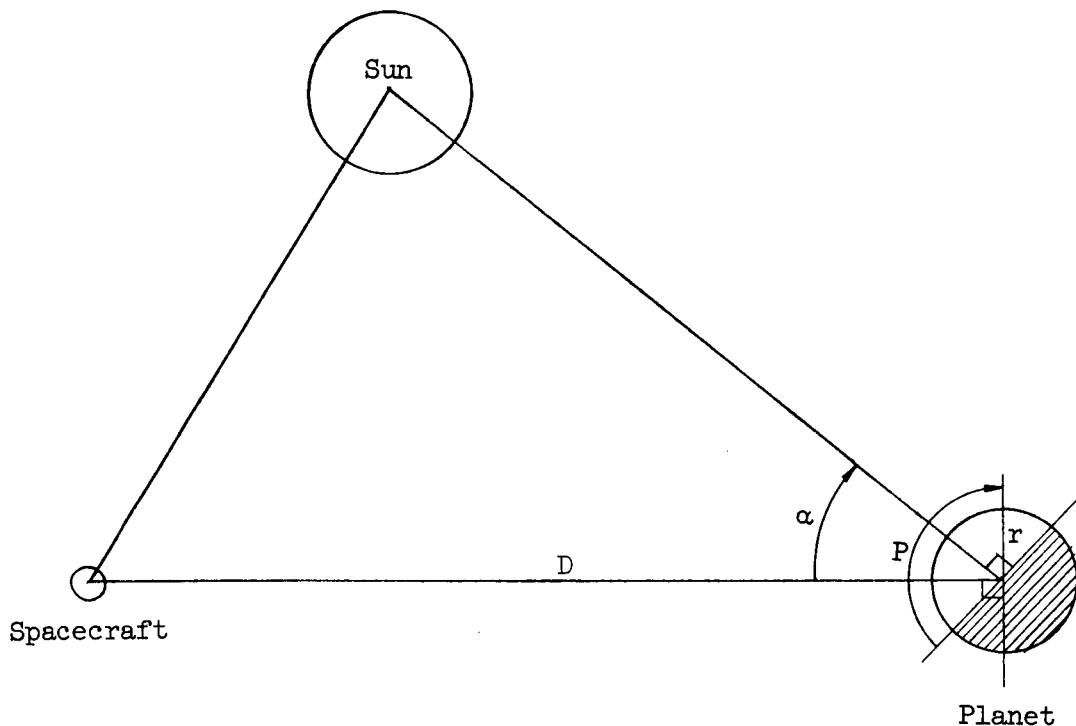
\vec{R}_{ebi} position vector from center of Earth to center of body i

\vec{R}_{ev} position vector from center of Earth to spacecraft

Planetary phases and eclipses.- In this study, the phase of the planet is defined as the ratio of the visible Sun-lighted portion of the planet to the total portion visible from the spacecraft. Under the assumption of spherical bodies, the calculation of phase may be reduced to a two-dimensional problem in

which the plane of reference is determined by the positions of the spacecraft, and the centers of the Sun and the planet.

In instances where the angular diameter of the planet is very small (less than 1°) the phase is adequately approximated by the ratio $d/2r$ where d is the projection of the lighted visible portion of the planet onto the planet diameter normal to the spacecraft line of sight as shown in the following sketch:



From this sketch it is seen that

$$\text{Phase} = \frac{r - r \cos P}{2r} = \frac{1 - \cos P}{2} \quad (8)$$

where

$$P = 180^\circ - \alpha$$

Whenever the angular diameter of Mars and Earth exceeded 1° a more exact procedure was used for calculating the phases of these two planets. Consider the following sketch, in which

$$\alpha_1 = 180^\circ - \alpha$$

$$P = \alpha_1 + \beta$$

then

$$\beta = M_1 - M_2$$

$$\text{Since } P = 180^\circ - \alpha + \beta = 180^\circ - \alpha + M_1 - M_2$$

$$\begin{aligned} P &= 180^\circ - \alpha + \frac{1}{2}(270^\circ - \alpha_1) - \text{arc tan} \left[\frac{r - c_1}{r + c_1} \tan \frac{1}{2}(270^\circ - \alpha_1) \right] \\ &= 180^\circ - \alpha + \frac{1}{2}(270^\circ - 180^\circ + \alpha) - \text{arc tan} \left[\frac{r - c_1}{r + c_1} \tan \frac{1}{2}(270^\circ - 180^\circ + \alpha) \right] \end{aligned} \quad (9)$$

or

$$P = 180^\circ - \alpha + \frac{1}{2}(90^\circ + \alpha) - \text{arc tan} \left[\frac{r - c_1}{r + c_1} \tan \frac{1}{2}(90^\circ + \alpha) \right] \quad (10)$$

Substituting

$$r_1 = (r^2 - c_1^2)^{1/2}$$

and

$$c_2 = (c_1^2 + r^2 - 2c_1r \cos \phi)^{1/2}$$

obtained by applying the law of cosines, in equation (10) yields

$$\text{Phase} = \frac{r_1 + c_2 \cos(180^\circ - P)}{2r_1} = \frac{r_1 - c_2 \cos P}{2r_1} \quad (11)$$

Planetary eclipses were determined by examination of the data giving phases, positions, and angular diameters of the solar-system bodies.

RESULTS AND DISCUSSION

By applying equations (1) to (11) to the Martian trajectory data the results presented in figures 2 to 8 were obtained.

The positions of the Earth and the spacecraft projected upon the star background of the Navigational Star Chart are shown in figure 2. The heavy dashed curve shows the position of the spacecraft as seen from the Earth (center); the solid curve gives the position of Earth as seen from the vehicle. Since the Earth-vehicle vector is the negative of the vehicle-Earth vector, the two curves are mirrored about the celestial equator with a shift of 180° in sidereal hour angle. The numbers with a subscript h on the curves denote flight time in hours from injection and the numbers without subscripts indicate flight time in days after exit from the sphere of influence of the Earth. Data of the type

shown on figure 2 could be used to provide radar-pointing predictions to Earth-based tracking stations.

The relatively rapid change in apparent position during the first few hours of flight occurs because the spacecraft is still traversing its escape parabola in the vicinity of its vertex and hence is partially circling the Earth. As the vehicle recedes farther from the Earth its direction of motion becomes more nearly straight away, with a resulting decrease in the rate of change of apparent position. Similar curves would result if the analogous Mars-vehicle situation were considered, except that the direction of change of apparent position would be reversed.

Apparent positions of the celestial bodies and the spacecraft as seen from Earth at the time of spacecraft exit from the sphere of influence of Earth are shown in figure 3(a). Figure 3(b) gives the positions of the Sun and planets on the celestial sphere as seen from the spacecraft at this same time. These two figures indicate that there is no appreciable change in the apparent positions of the celestial bodies at this time whether viewed from the Earth or the vehicle. This is due to the shift in reference position (approximately 845,000 km) being insignificant in comparison with the great distances separating the bodies of the solar system.

Figures 3(c) and 3(d) show the positions of the celestial bodies, at the time of vehicle entry into the sphere of influence of Mars ($T = 185$ days), as seen from the Earth and the vehicle, respectively. Comparison of these two figures shows appreciable changes in apparent positions of the Sun and the inner planets, since the shift in reference position is of a magnitude comparable to the separation distances between these bodies. The outer planets show little displacement in apparent position since the reference shift is still minor with respect to the distance between these bodies and the Earth-vehicle system.

In figure 4, the projection of the spacecraft heading on the star background is shown. Such a projection would help the pilot in alining the spacecraft attitude with the flight path.

Figures 5(a) to 5(c) show the traces of the positions of the solar-system bodies on the celestial sphere as seen from the vehicle during the 185-day heliocentric phase of the mission. It is noted that the only significant changes in apparent position are experienced by the Sun and the inner planets. All bodies, with the exception of Earth (at the beginning of the mission) and Mars (during the final phase of the mission), lie approximately on the ecliptic. Rapid change in the apparent position of Mars is noted during the final portion of the heliocentric phase as shown in figure 5(a). Energy considerations restrict the vehicle trajectory to a region close to the ecliptic plane and thus permit large deviations from the ecliptic in planetary apparent position only when the spacecraft is in the immediate vicinity of the observed planet. (Pluto is excluded from this consideration but it is doubtful that this small, distant body has any navigational value for the type of mission investigated.) Preflight analysis of the type of data shown in figure 5 would determine what combinations of celestial bodies would be most suitable for navigation purposes on a particular mission. Thus large-scale navigational maps to be used during

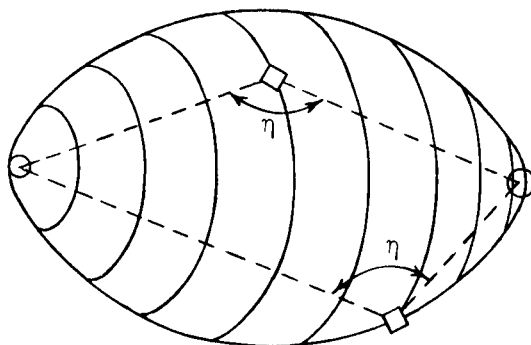
the flight need be made only of the specific areas of interest for that particular mission.

For the specific Earth-Mars trajectory considered it is seen that no star of navigational importance is occulted by any of the solar-system bodies during the heliocentric phase. Although such occultations are possible the combination of extremely small planetary angular diameters and the restriction of planetary apparent position to a narrow band bordering the ecliptic make their occurrence improbable.

The angular diameter of Earth during the geocentric portion of the flight is shown in figure 6(a). Figures 6(b) and 6(c) illustrate the variations in angular diameter of the solar-system bodies during the heliocentric phase. The angular diameters of the solar-system bodies, excluding Earth, are essentially constant during the geocentric phase of flight and can be taken as the initial values given in figures 6(b) and 6(c) for the heliocentric phase.

Figure 7 consists of plots of the included angle between various pairs of the solar-system bodies as measured from the vehicle. It is obvious that the included angle will show the greatest variation for pairs of bodies having the greatest change in apparent position. Thus it can be inferred (from fig. 5) that variations in included angle will be greatest when at least one of the bodies under consideration is either the Sun or an inner planet and that the included angle between pairs of outer planets should remain approximately constant. This inference is borne out by figures 7(b) to 7(g). The information given in figure 7 could be used during flight to preset a sextant with sufficient accuracy to locate the two bodies under consideration within the field of view. Plots of the type shown in figure 7 also give information that may be of navigational significance, such as the occurrence of included angles of 0° and 180° .

An illustration of the value of these particular angles is found in the problem of obtaining a position fix in space. An observed angle greater than 90° between two planets fixes the spacecraft's position on an ellipsoidal shaped surface. This surface is illustrated in the following sketch:



For the special cases in which the measured angle is either 0° or 180° the surface of position converges to a line of position. (Consider, for example, the

angle included between Venus and Uranus (fig. 7(e)) at $T = 41$ days.) In either of these cases a second angle measurement between either planet and a third is sufficient to determine the location of the spacecraft on the line of position. Thus a position fix may be obtained with two angle measurements whereas, in general, more measurements would be required. (See ref. 3.)

Figure 8 illustrates planetary phases as functions of flight time. Only the variations in Earth phase during the geocentric portion of the mission are shown in figure 8(a) since the phases of the other planets are essentially constant during this relatively short time period. Figure 8(b) illustrates that the rate of planetary phase change is primarily dependent upon the nearness of the planet to the Sun since, in general, the smaller the radius of the planet's orbit, the greater the time rate of change of the Sun-planet-vehicle configuration. Exceptions to this generality occur when the vehicle is close to one of the planets as illustrated by the rapid change in Earth phase during geocentric flight.

Although planetary phases as predicted by geometry may be extremely difficult to observe, because of large distances and distortion by cloud cover, and hence have little navigational importance in their own right, they do affect angle measurements. For example, consider a sighting of the planet Venus from near Earth when Venus is at its brightest. Since apparent brightness is a function of both distance and phase, Venus is brightest in the crescent phase, not when full. (See ref. 8.) Unless considerable magnification is used Venus will appear as a point source of light even in the crescent phase. Thus a sighting centered on this point source will yield angle measurements for the position of Venus which are several arc-seconds in error from the true position. Knowledge of planetary phases as a function of flight time will permit corrections to be made for this source of error. It may be noted that the phases of all planets exterior to Mars remain essentially full during the entire flight. This will hold true for any mission in which the vehicle trajectory remains within or near the Mars orbit since for this geometry it is impossible for planets exterior to Mars to exhibit phases other than gibbous phase.

Cross-reference between figures 5, 6, and 8 provides adequate information to describe completely the occultation of one solar-system body by another. As an illustration of this procedure consider occultations of Mercury by the Sun. Although the angular diameters of all bodies of the solar system are less than 1° throughout the heliocentric phase, it is seen in figure 7(c) that either occultations or transits of Mercury may occur after 12, 57, 121, and 165 days of heliocentric flight. Referring to figure 8(b) shows that the phase of Mercury is full at 12 and 121 days and new at 57 and 165 days. Since the phase of a planet orbiting interior to the vehicle trajectory is full when aligned with the vehicle and the Sun if the Sun is between the planet and the vehicle, occultations of Mercury by the Sun occur at 12 and 121 days. At 57 and 165 days Mercury is in transit across the Sun. Comparison of angular diameters as shown in figure 6 determines the degree to which one body is occulted by the other. Figures 6 and 7 (or enlargements of these) could be used to determine the length of time that one body is partially or totally occulted by the other.

CONCLUDING REMARKS

A preliminary study of some of the geometric phenomena of space flight as seen from a spacecraft has been conducted. The specific quantities studied for a typical Earth-Mars trajectory were: positions of the Sun and planets on the celestial sphere, the trace of the vehicle heading on the celestial sphere, angular diameters of the bodies of the solar system, included angles between pairs of these bodies, and planetary phases and eclipses. The report also presents the method and pertinent equations for determining these geometric phenomena. Results shown for the mission to Mars discussed herein would, in general, apply to other interplanetary missions and could be extended to include certain navigational stars. An investigation of this type would yield information useful in the preflight planning of onboard navigational procedures such as selection of the most suitable combinations of celestial bodies for particular measurements and the preparation of large-scale flight maps of the specific regions of the celestial sphere of interest for a given mission. This information could also be used during flight to preset angle-measuring devices to precalculated values and thus reduce the navigator's work to fine adjustments when making the actual measurement.

The results obtained in this study, as well as some implied results and applications, are summarized as follows:

1. During the departure and approach phases of an interplanetary mission, while the spacecraft is within the sphere of influence of the launch or target planet, the quantities showing most significant rates of change are those with respect to this primary planet.
2. During the heliocentric phase of the mission, variations in the geometric quantities considered were much greater for the inner planets; the variations were largest for Mercury and became extremely small for planets beyond Jupiter.
3. The extremely small values of angular diameter and their slow rates of change during the heliocentric phase indicate that such measurements would be of little navigational importance for this phase except for presetting certain navigational instruments. However, the reverse is true for planetary approach or departure during which the angular diameter is large and changes rapidly; this phenomenon presents a means of determining distance and velocity relative to the primary planet.
4. Occultation of celestial bodies of navigational importance by bodies of the solar system during the heliocentric phase is, in general, a very rare occurrence.
5. The phases of all planets exterior to Mars remain essentially full and constant throughout the flight.

Langley Research Center,
National Aeronautics and Space Administration,
Langley Station, Hampton, Va., March 26, 1965.

REFERENCES

1. Battin, Richard H.: A Statistical Optimizing Navigation Procedure for Space Flight. Rep. R-341 (Contracts NAS-9-103 and NAS-9-153), Instrumentation Lab., M.I.T., Sept. 1961.
2. White, John S.; Callas, George P.; and Cicolani, Luigi S.: Application of Statistical Filter Theory to the Interplanetary Navigation and Guidance Problem. NASA TN D-2697, 1965.
3. Mayo, Alton P.; Hamer, Harold A.; and Hannah, Margery E.: Equations for Determining Vehicle Position in Earth-Moon Space From Simultaneous Onboard Optical Measurements. NASA TN D-1604, 1963.
4. Anon.: Planetary Co-ordinates for the Years 1960-1980 Referred to the Equinox of 1950.0. H.M. Nautical Almanac Office, 1958.
5. Anon.: Air Navigation. H.O. Pub. No. 216, U.S. Dept. Navy, 1955.
6. Pines, Samuel; and Wolf, Henry: Interplanetary Trajectory by the Encke Method Programmed for the IBM 704 and 7090. Rept. No. RAC-656-451 (Contract NASW-109 (NASA)), Rep. Aviation Corp., Dec. 12, 1960.
7. Kopal, Zdeněk: Numerical Analysis. John Wiley & Sons, Inc., 1955.
8. Payne-Gaposchkin, Cecilia: Introduction to Astronomy. Prentice-Hall, Inc., c.1954.

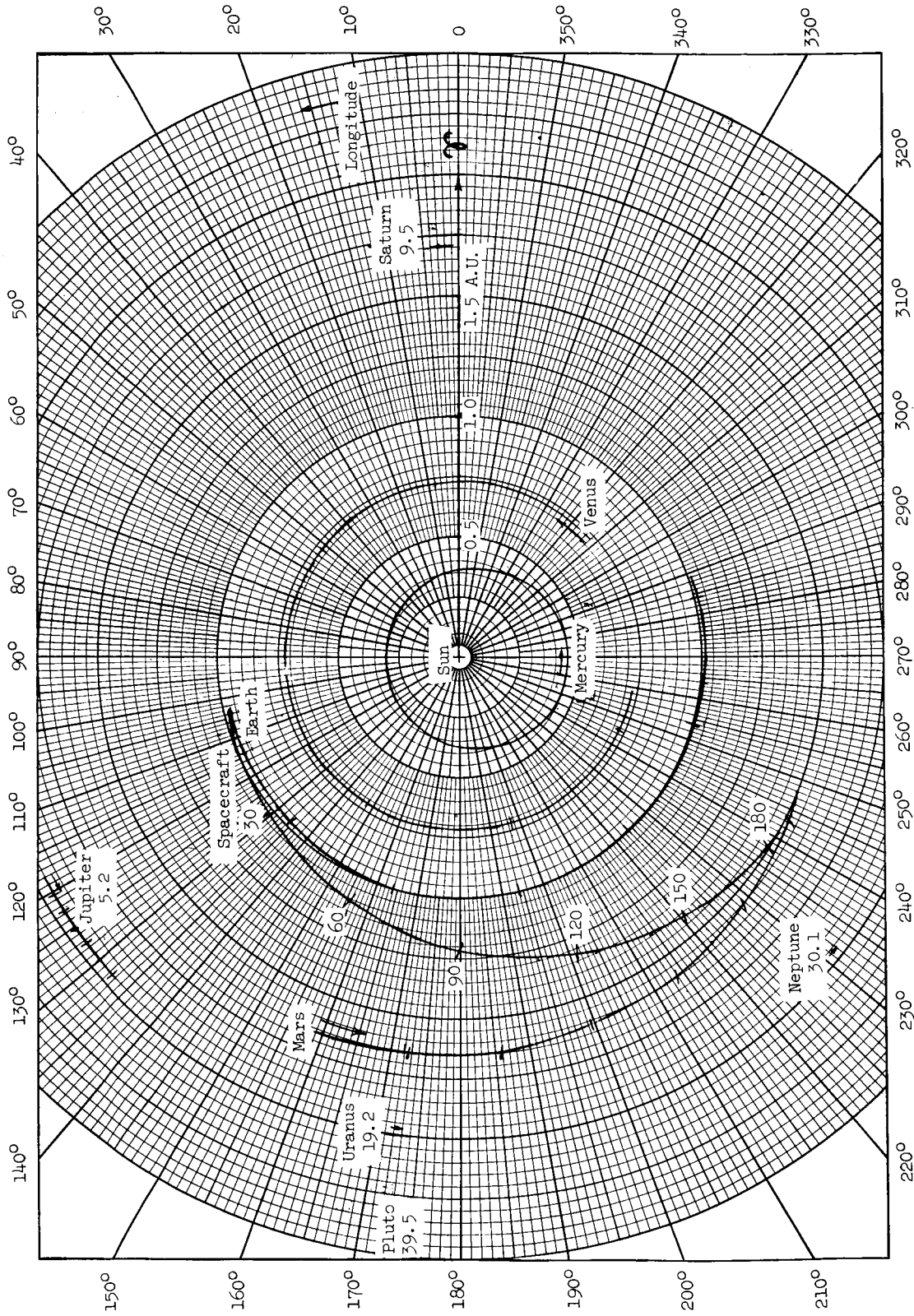


Figure 1.- Schematic of spacecraft and planet positions in Sun-centered equatorial-coordinate system during specified mission to Mars as viewed from north. Radii of inner planets only are drawn to scale; mean radii of outer planets are given in astronomical units (A.U.). Ticks indicate 30-day intervals.

NAVIGATIONAL STAR CHART

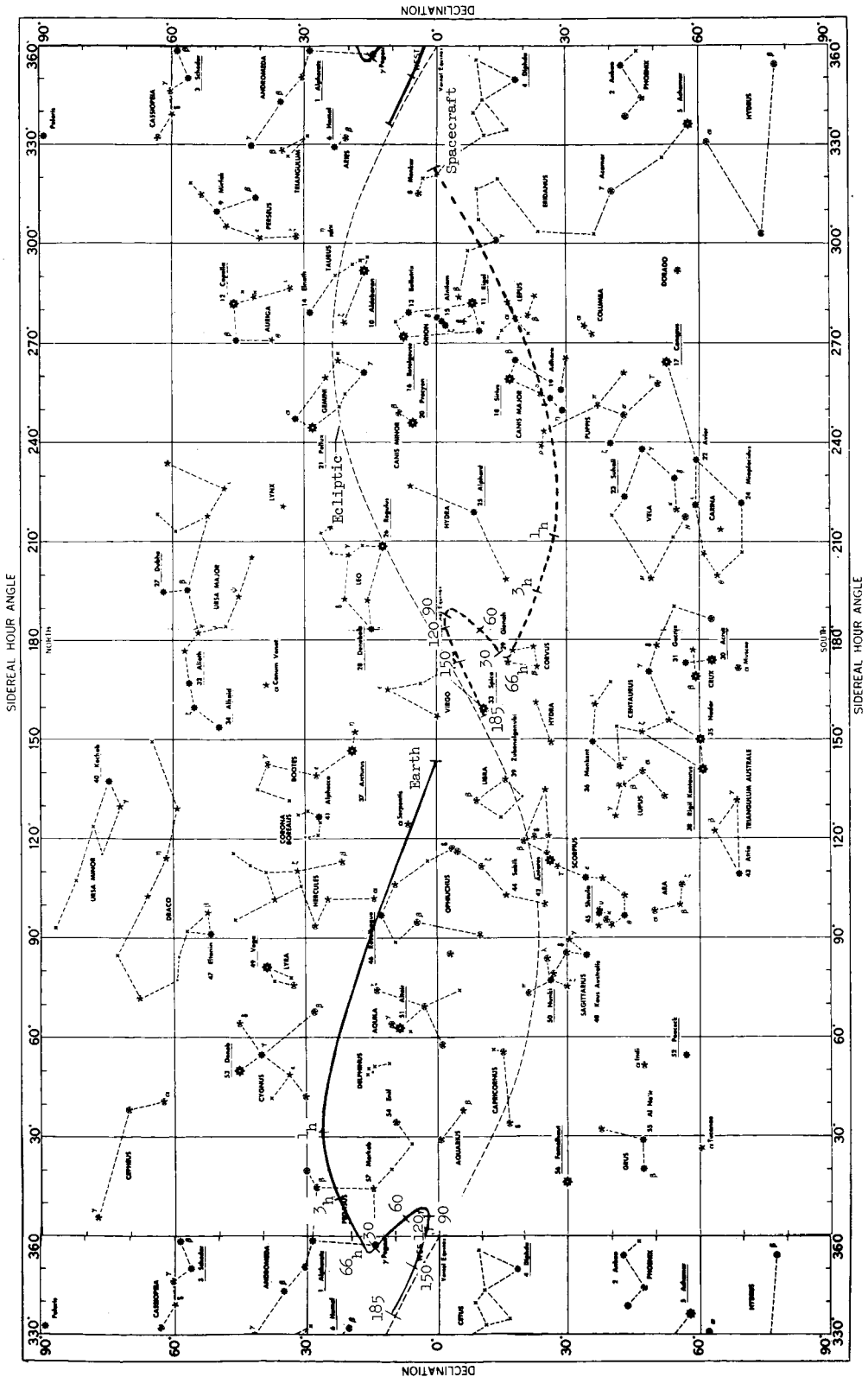
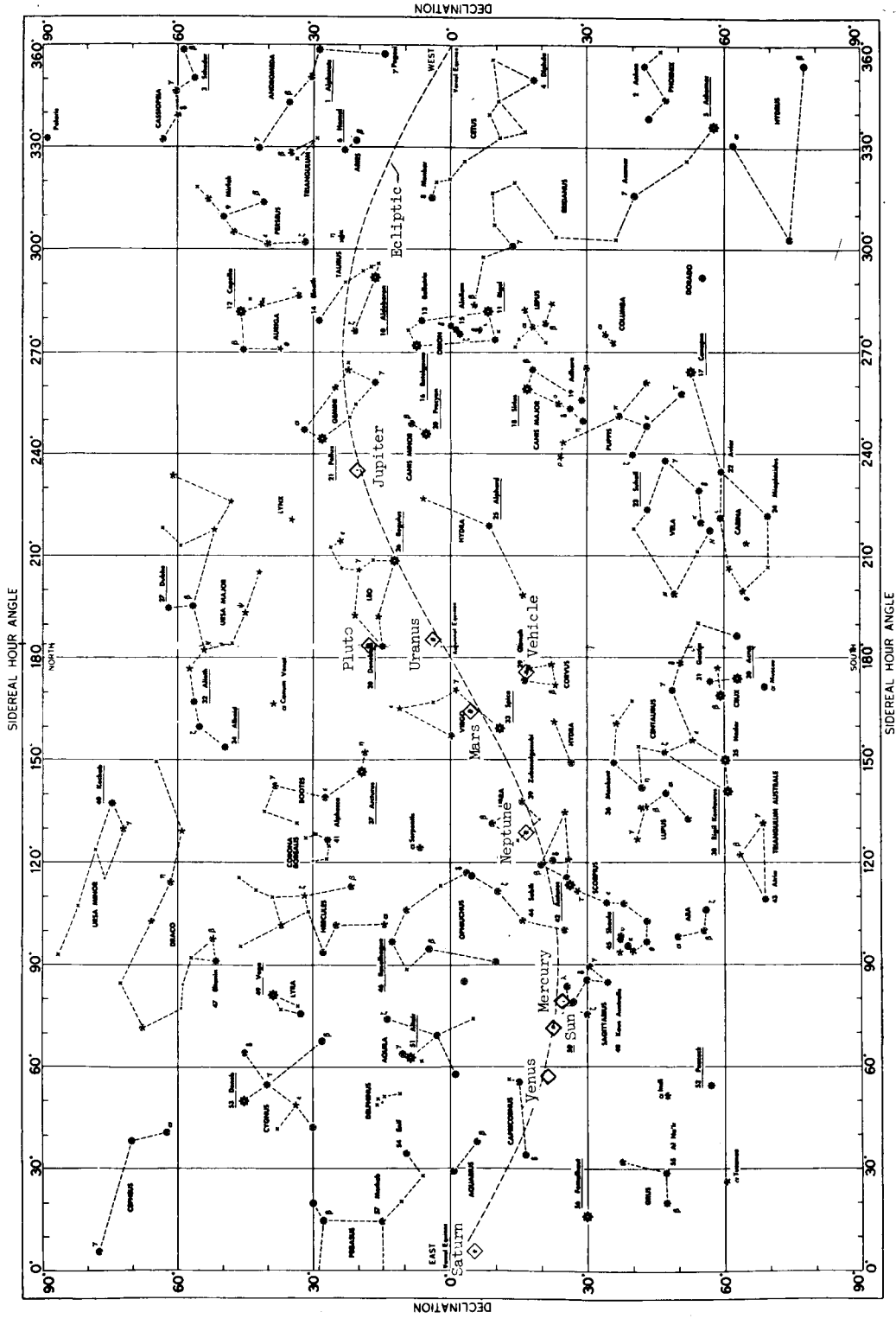


Figure 2.- Projection on Navigational Star Chart of position of Earth as seen from spacecraft (solid line) and position of spacecraft as seen from Earth (heavy dashed line).

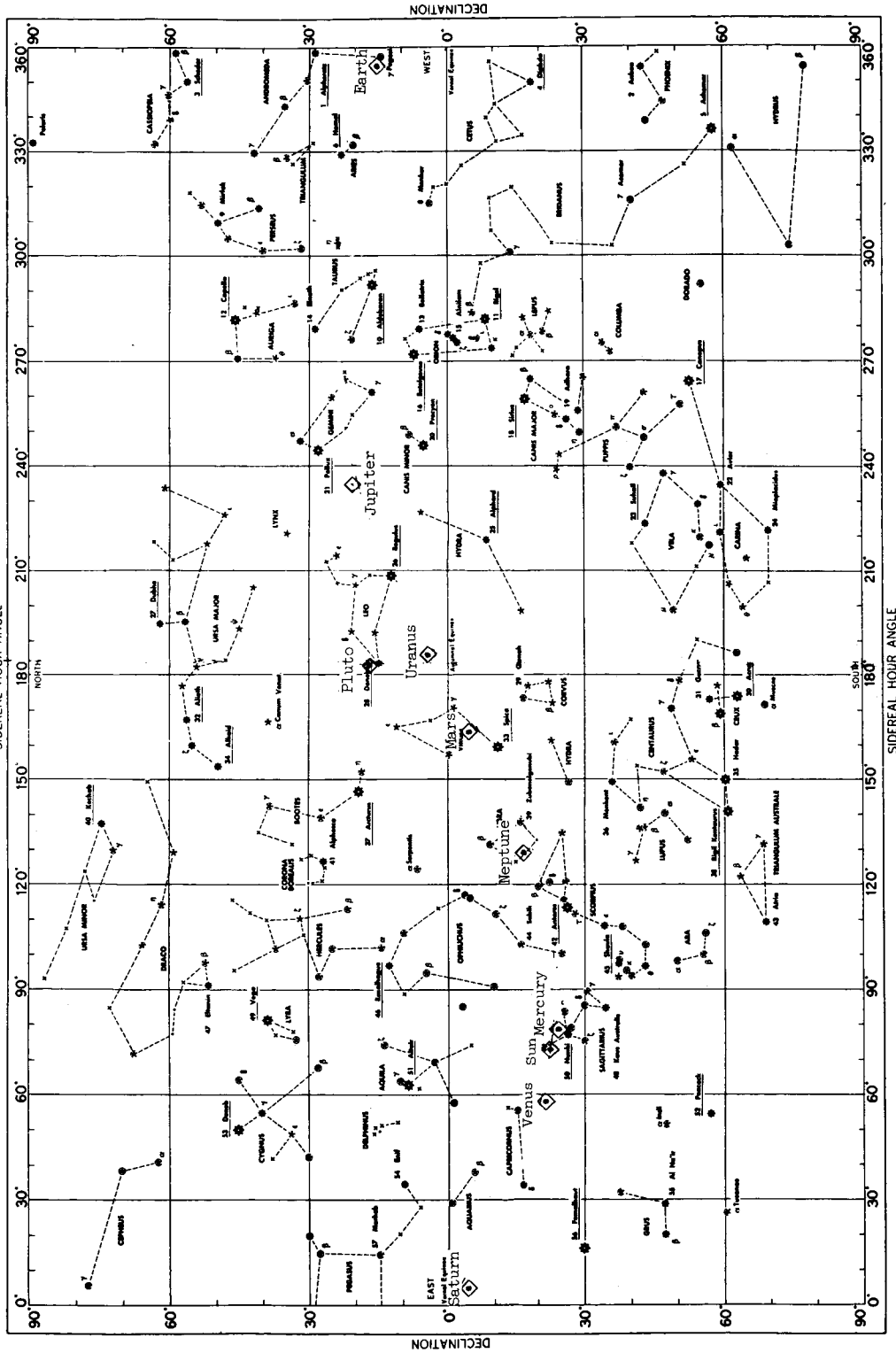
NAVIGATIONAL STAR CHART



(a) Positions of planets, spacecraft, and Sun as seen from Earth at time of spacecraft exit from sphere of influence of Earth.

Figure 3.- Projection on Navigational Star Chart of spacecraft and celestial bodies.

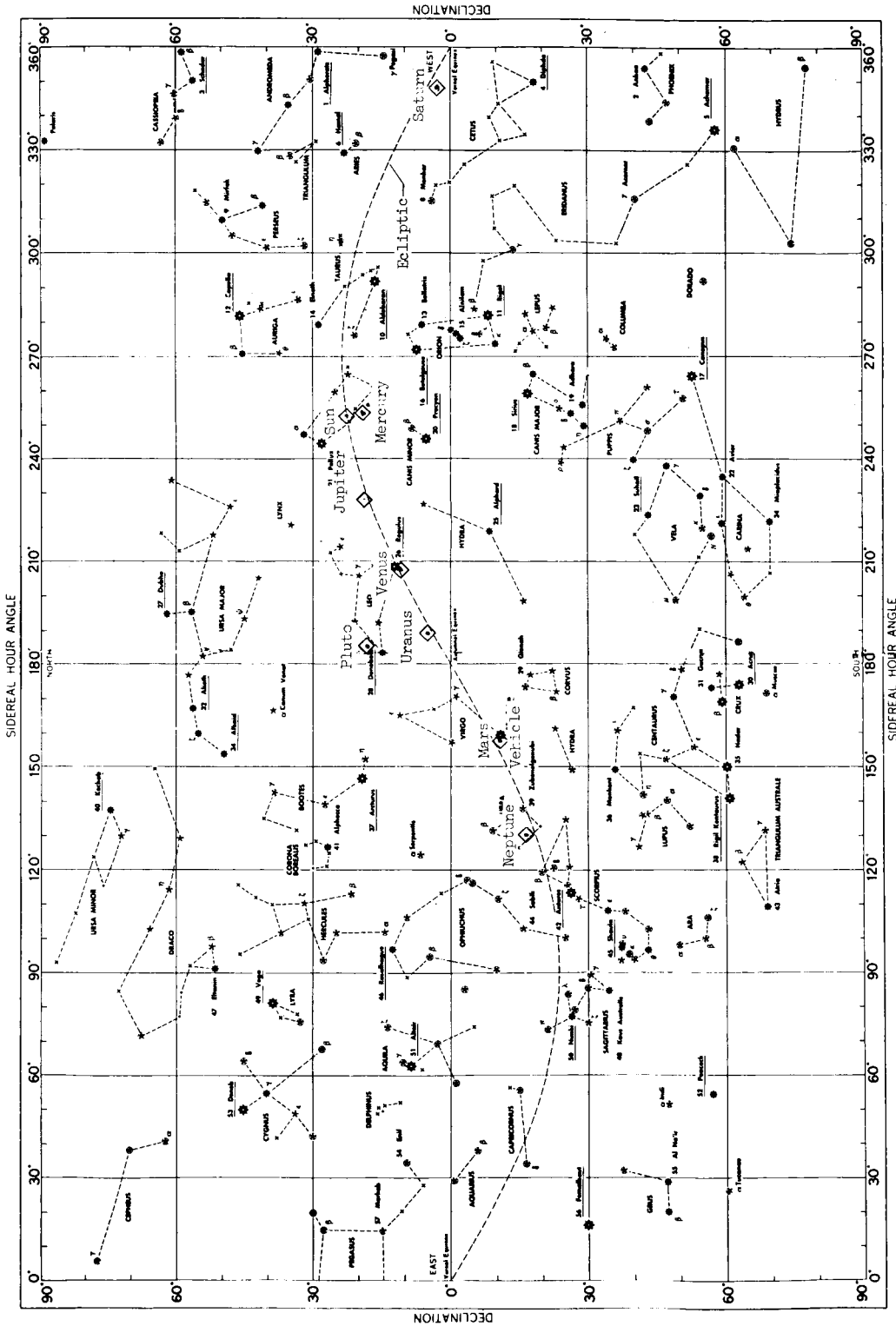
NAVIGATIONAL STAR CHART



(b) Positions of planets and Sun as seen from spacecraft at time of exit from sphere of influence of Earth.

Figure 3.- Continued.

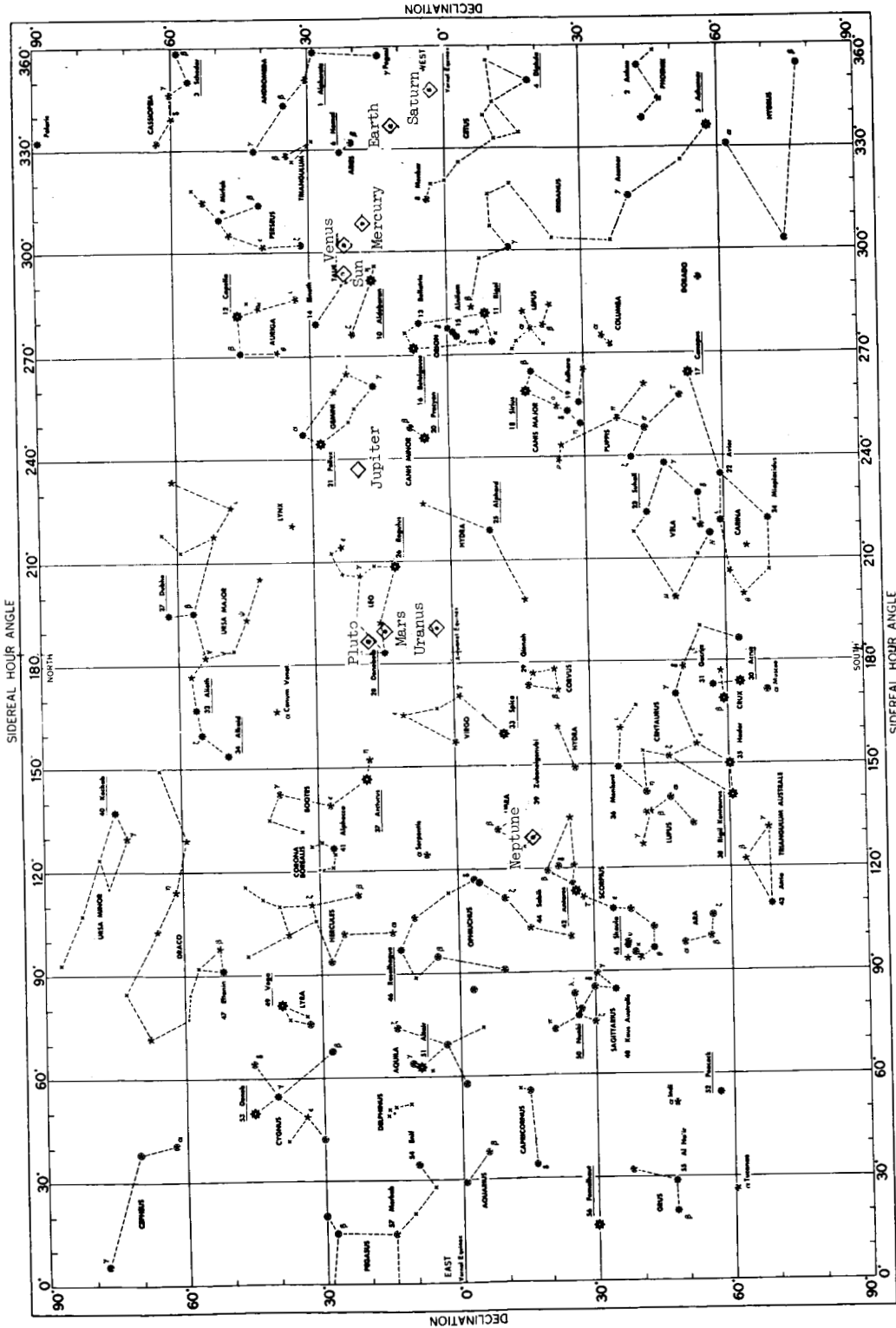
NAVIGATIONAL STAR CHART



(c) Positions of planets, spacecraft, and Sun as seen from Earth at $T = 185$ days.

Figure 3.- Continued.

NAVIGATIONAL STAR CHART



(d) Positions of planets and Sun as seen from spacecraft at $T = 185$ days.

Figure 3.- Concluded.

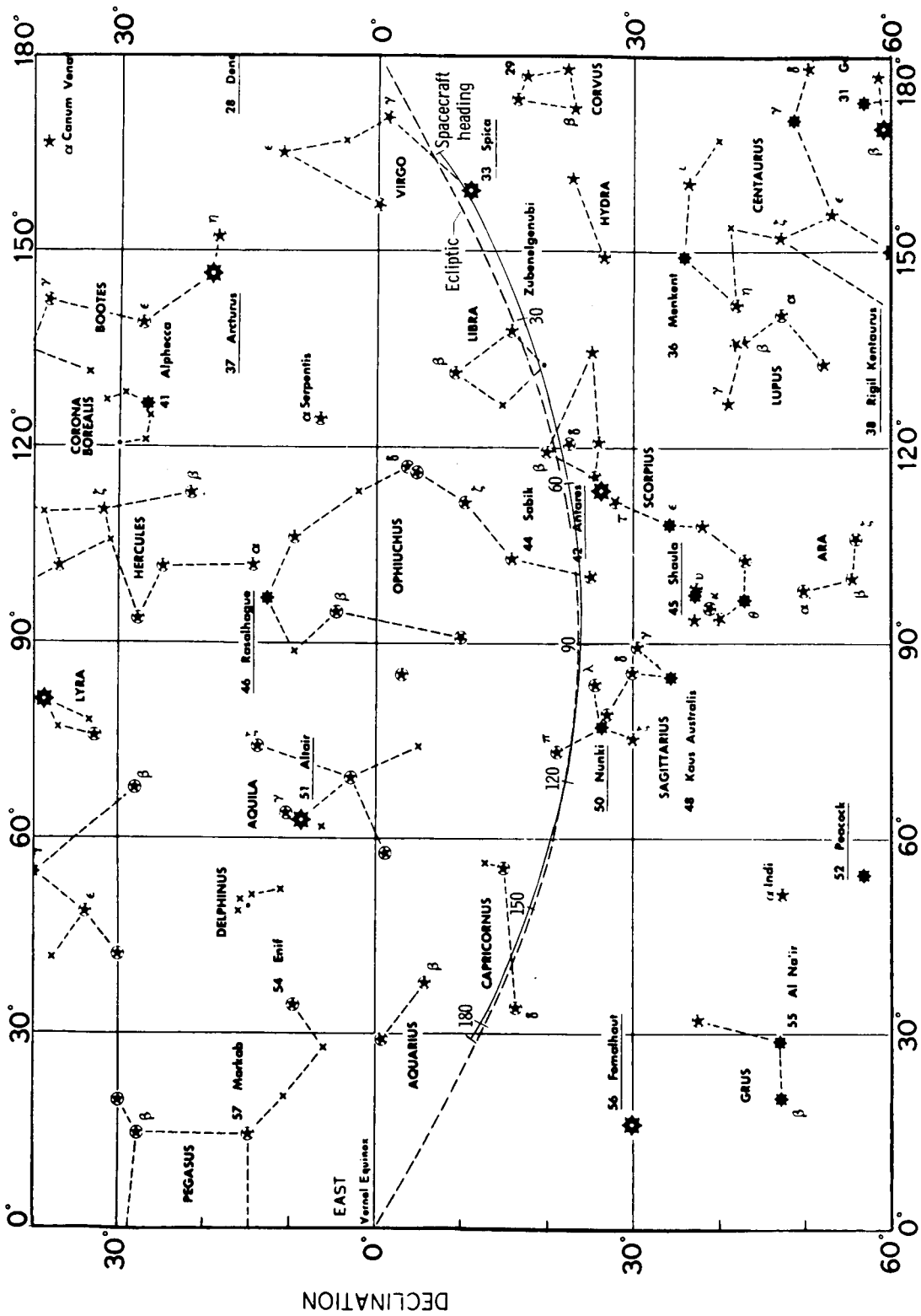
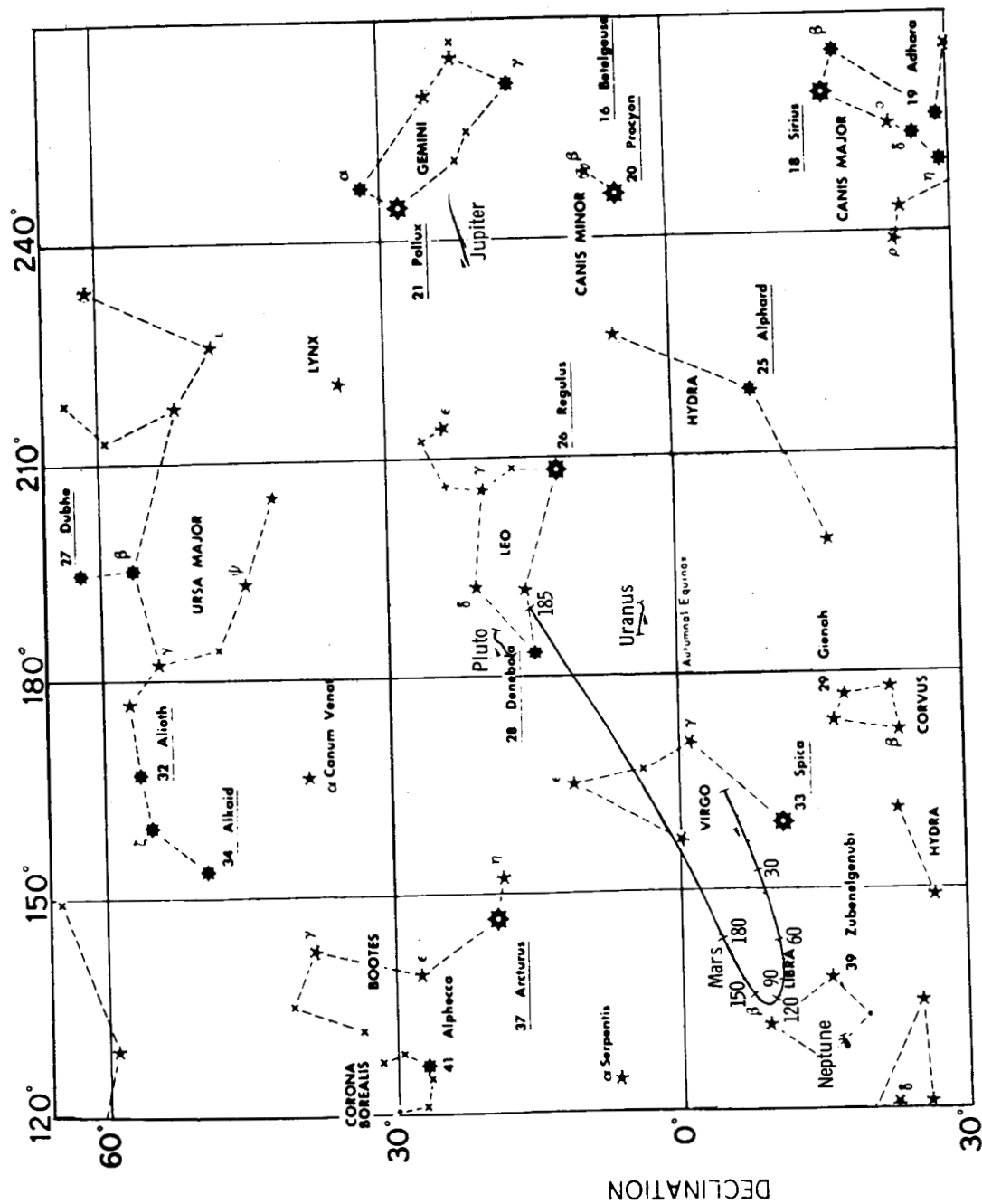
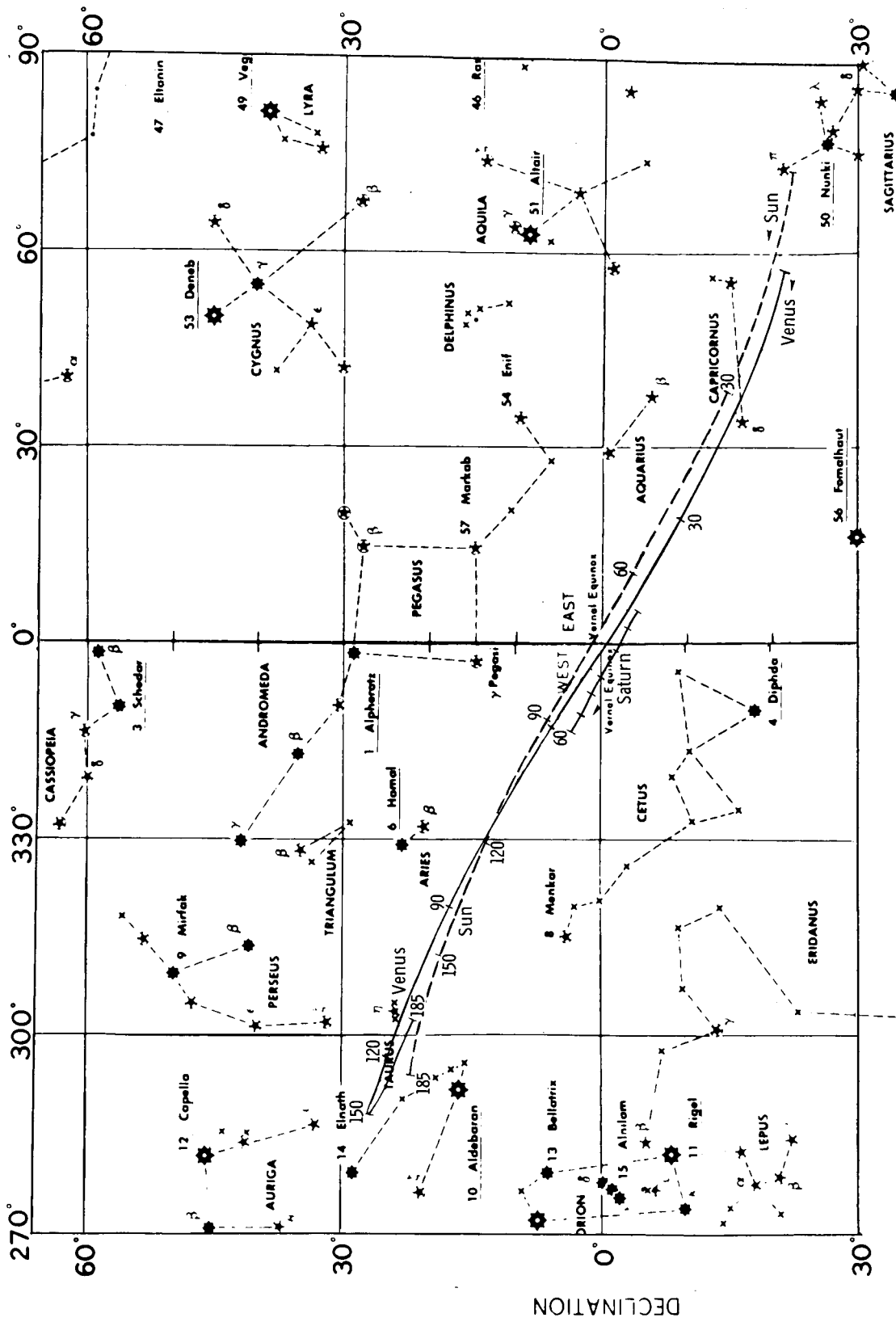


Figure 4.- Trace of spacecraft heading on star background.



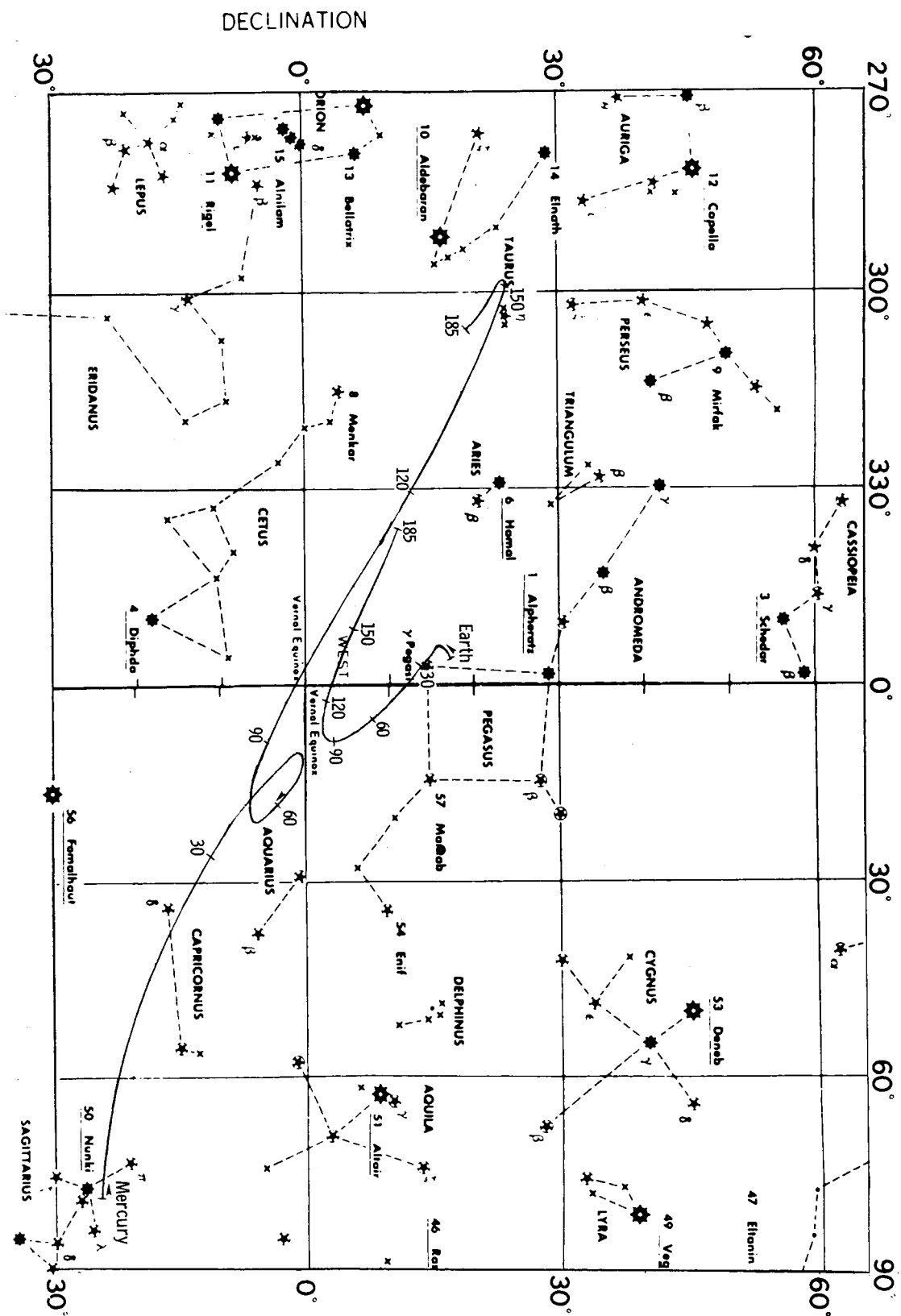
(a) Neptune, Mars, Uranus, Pluto, and Jupiter.

Figure 5.- Trace of planet positions on star background as seen from spacecraft during heliocentric phase of mission.



(b) Venus, Saturn, and Sun.

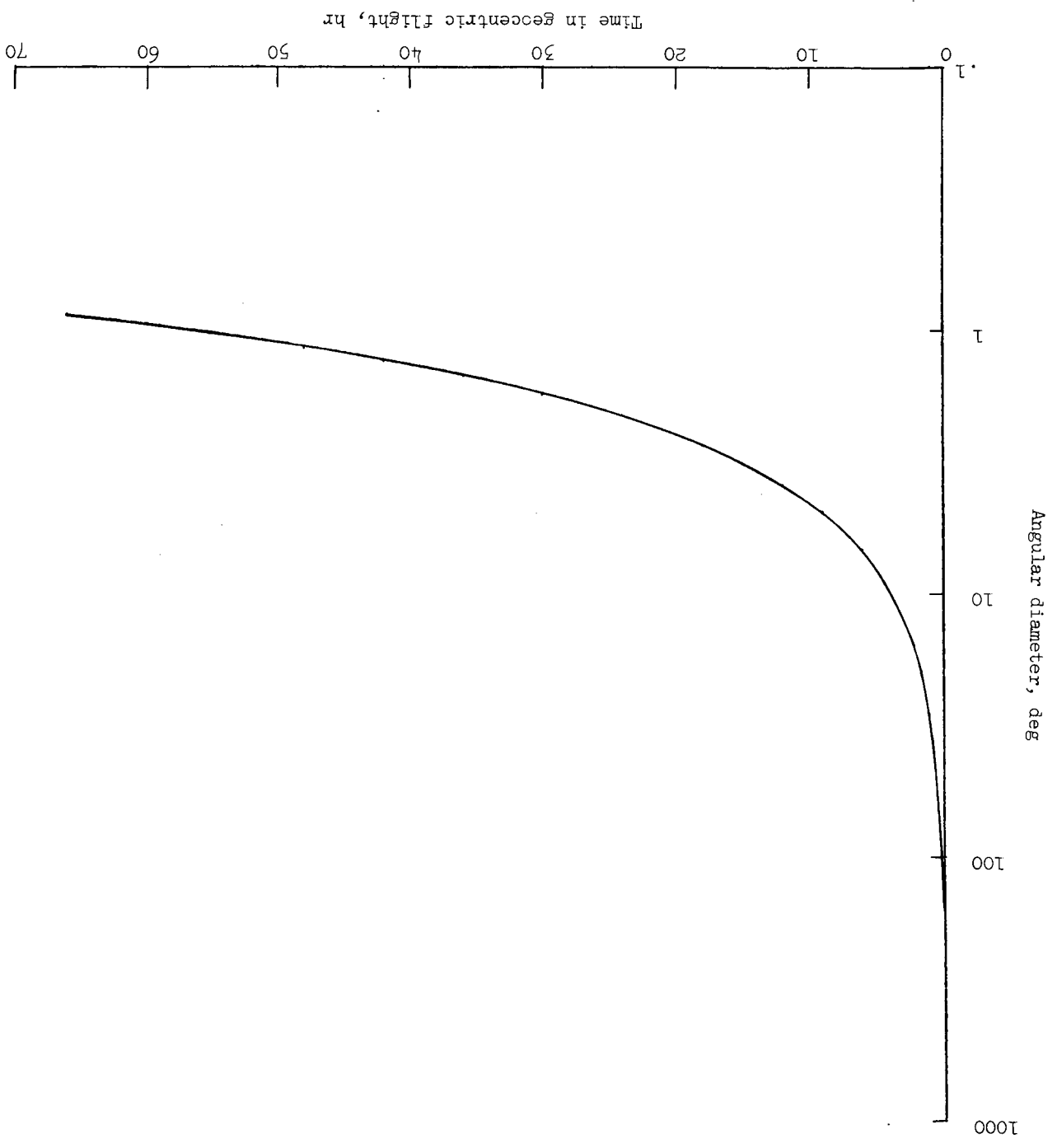
Figure 5.- Continued.

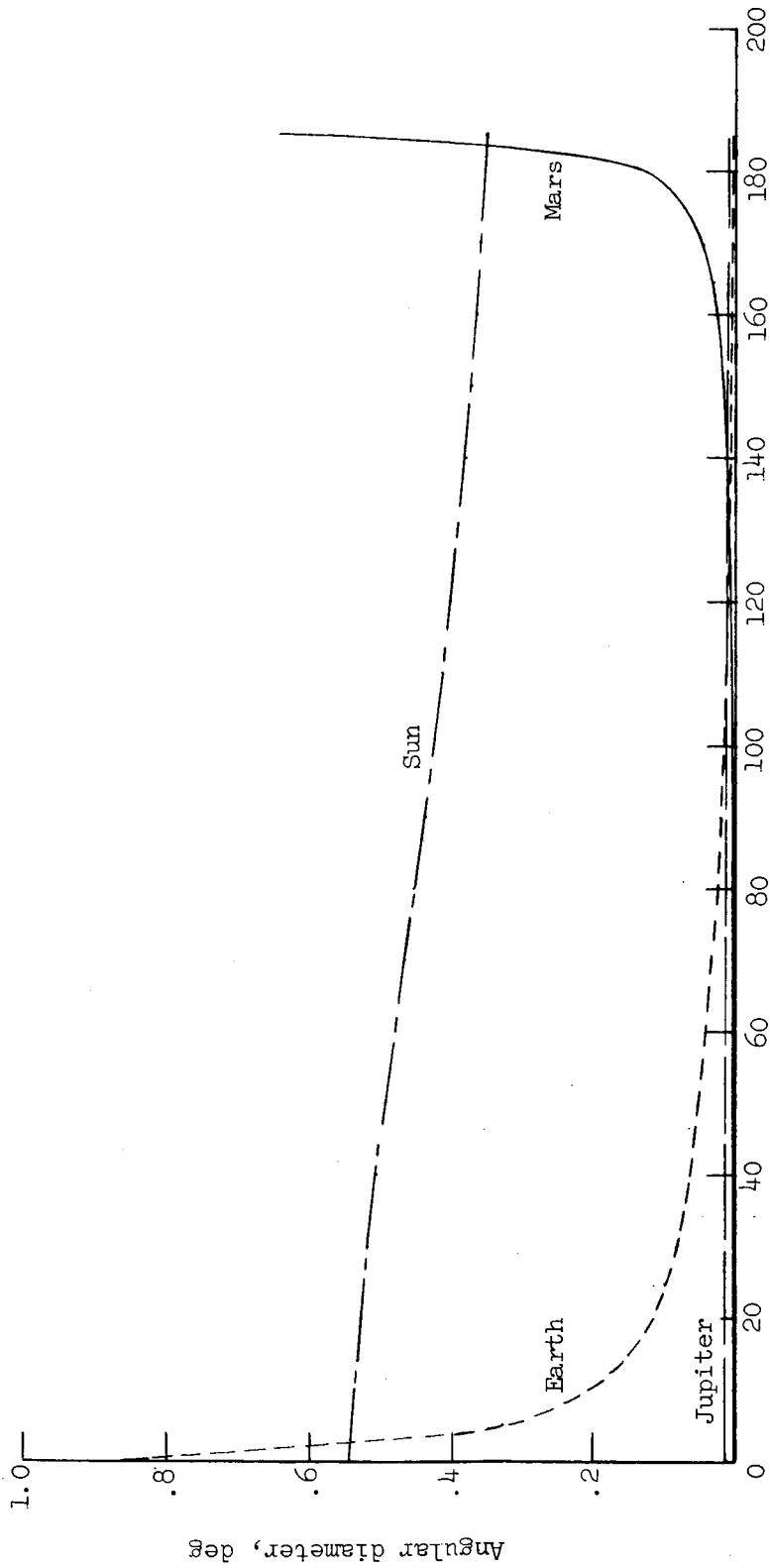


(c) Earth and Mercury.
Figure 5.- Concluded.

Figure 6.- Angular diameter of planets and Sun as viewed from spacecraft.

(a) Earth during geocentric phase of mission.

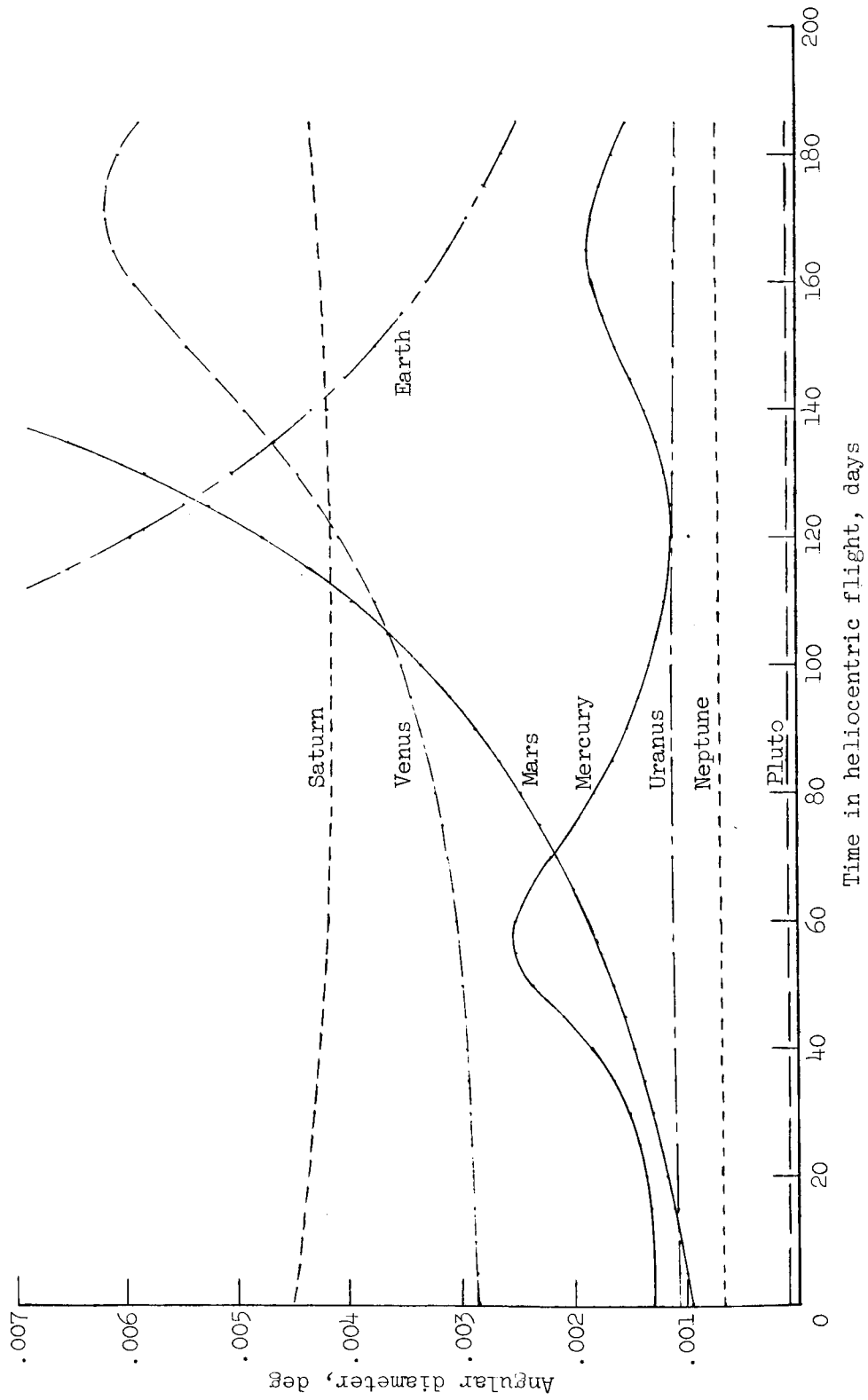




Time in heliocentric flight, days

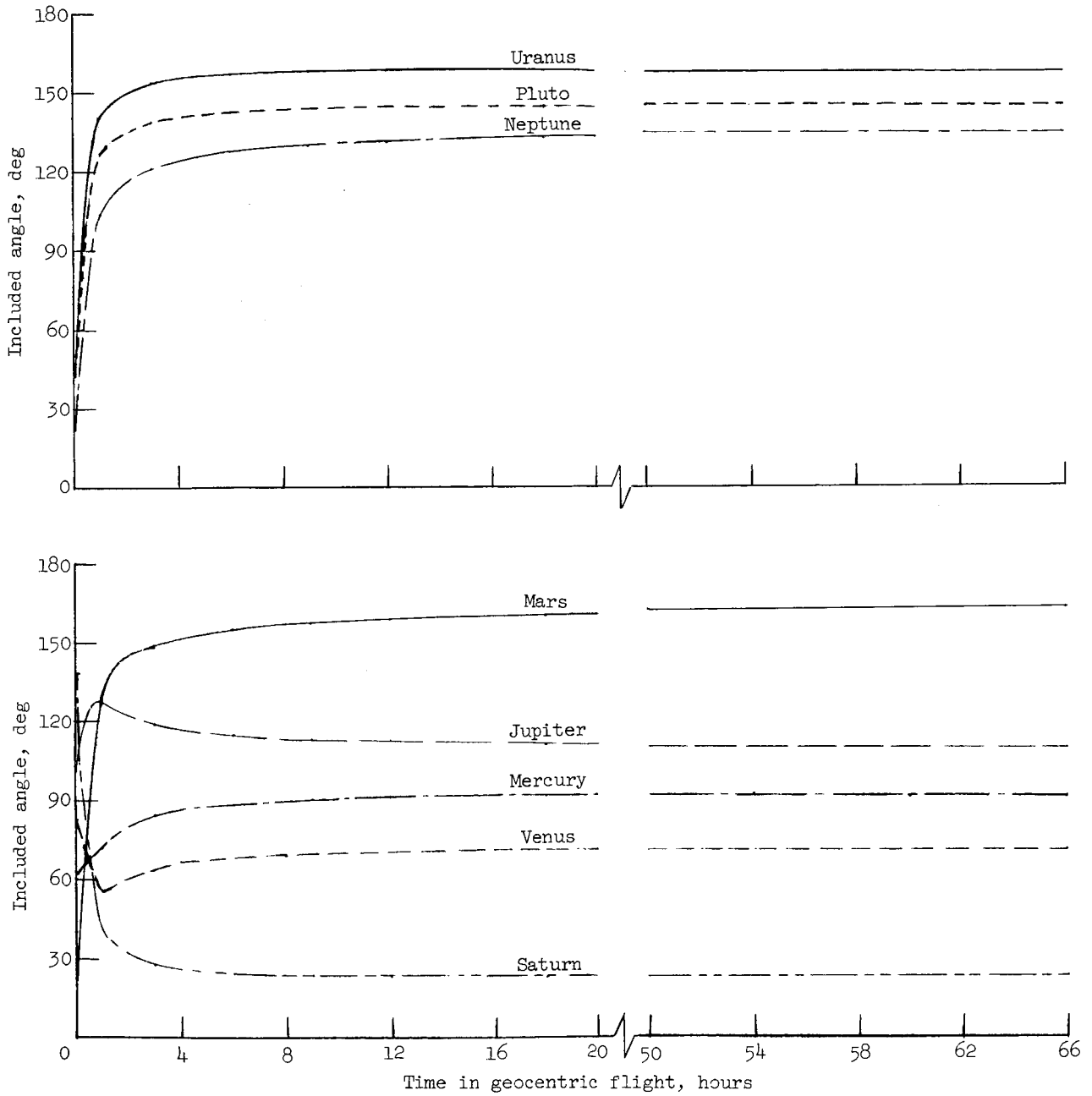
(b) Earth, Sun, Mars, and Jupiter.

Figure 6.- Continued.



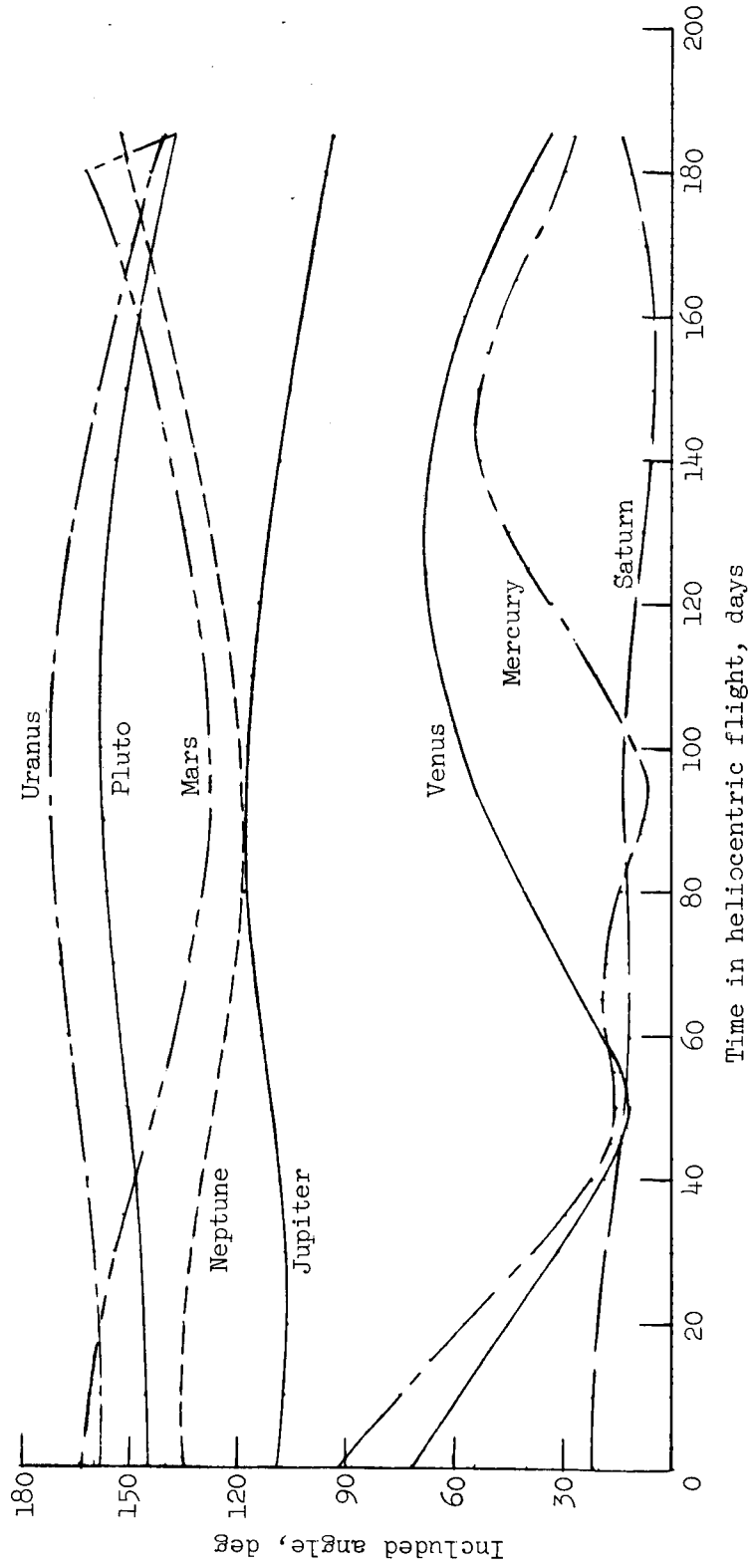
(c) Planets.

Figure 6.- Concluded.



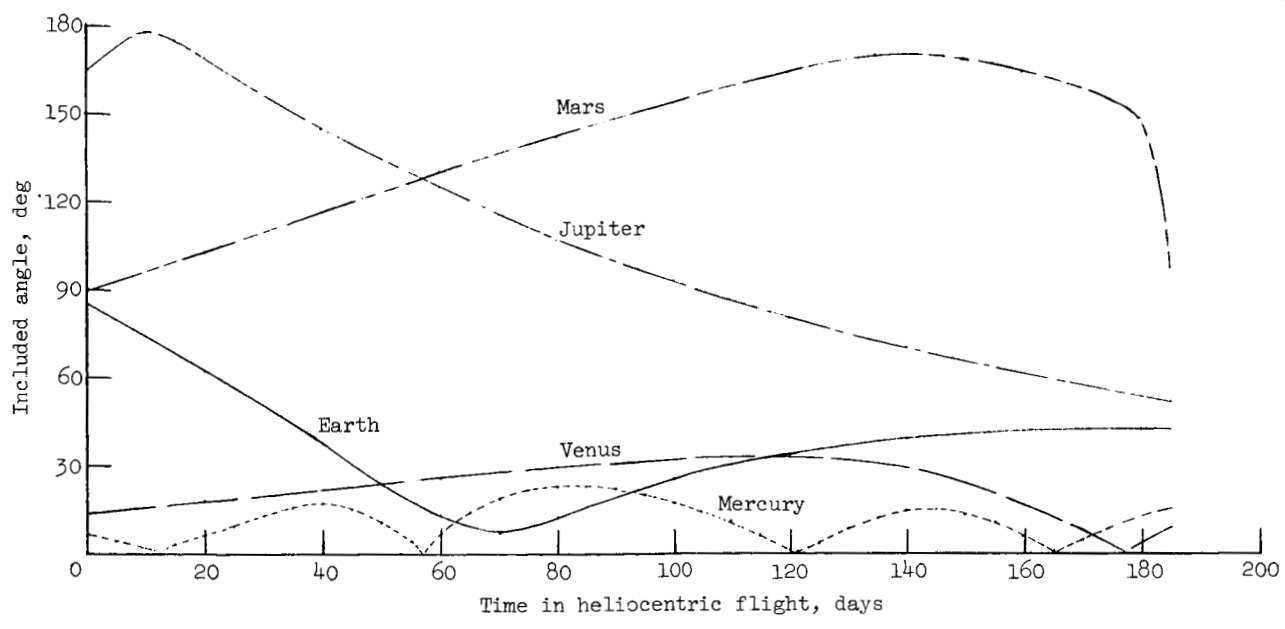
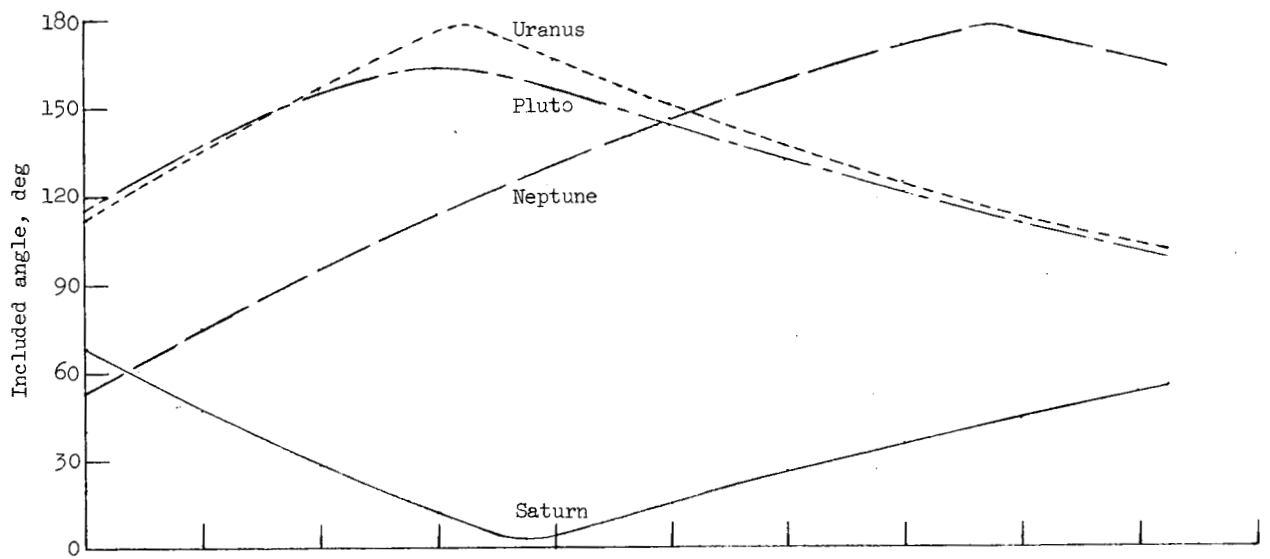
(a) Between Earth and other planets during geocentric flight.

Figure 7.- Angle included at spacecraft between various pairs of solar bodies.

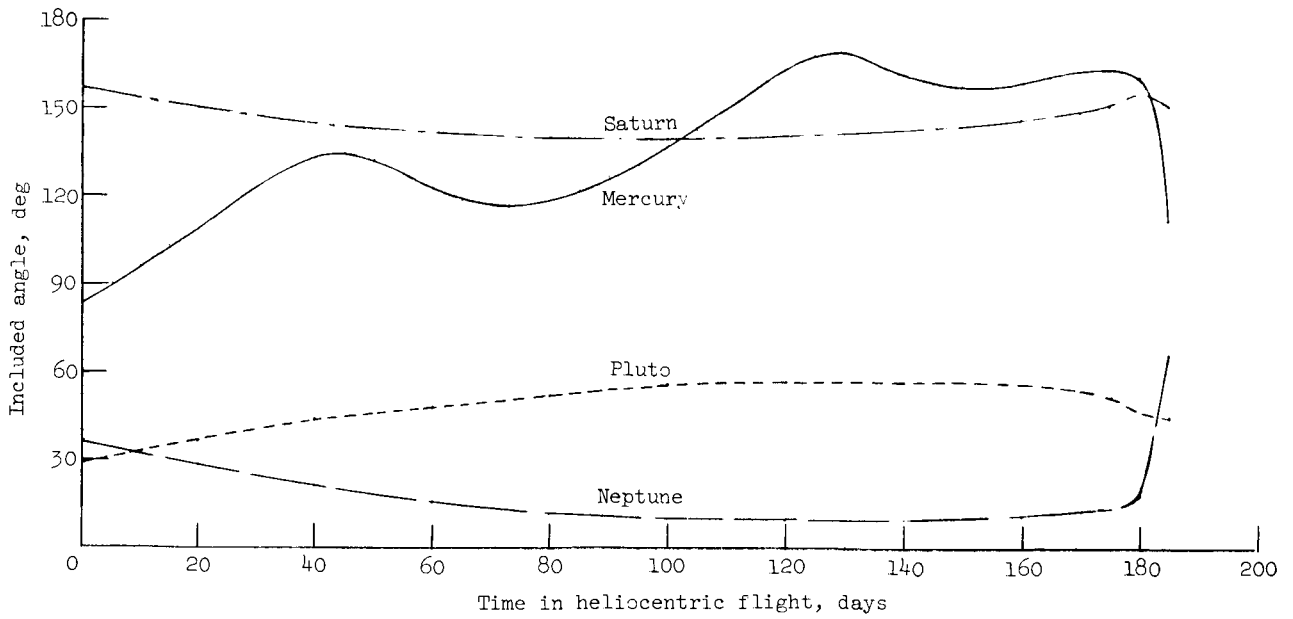
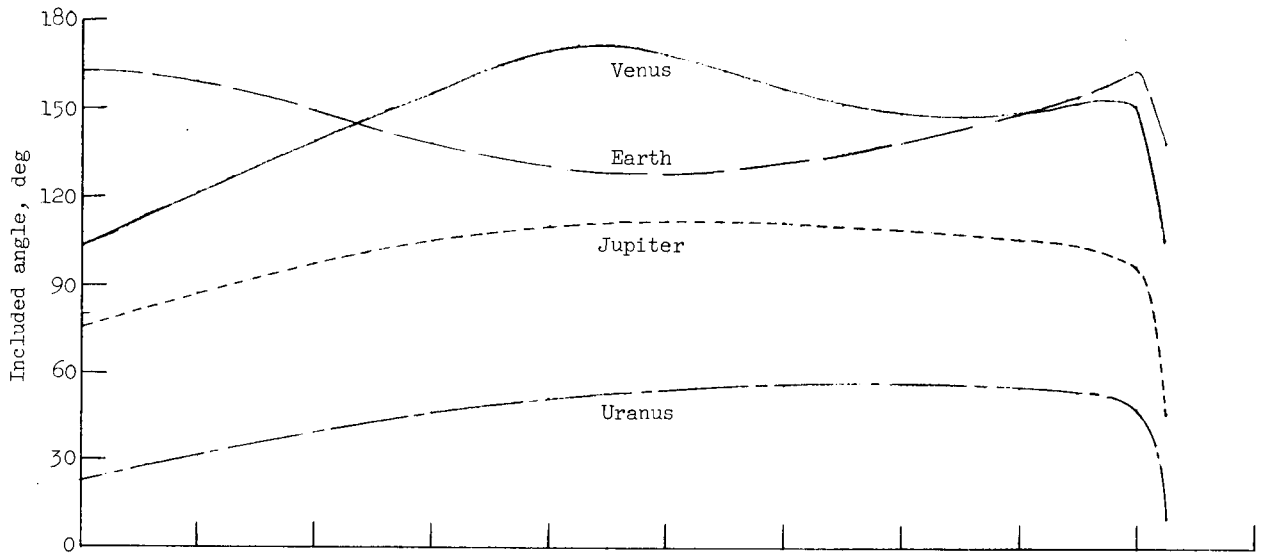


(b) Between Earth and other planets during heliocentric flight.

Figure 7.- Continued.

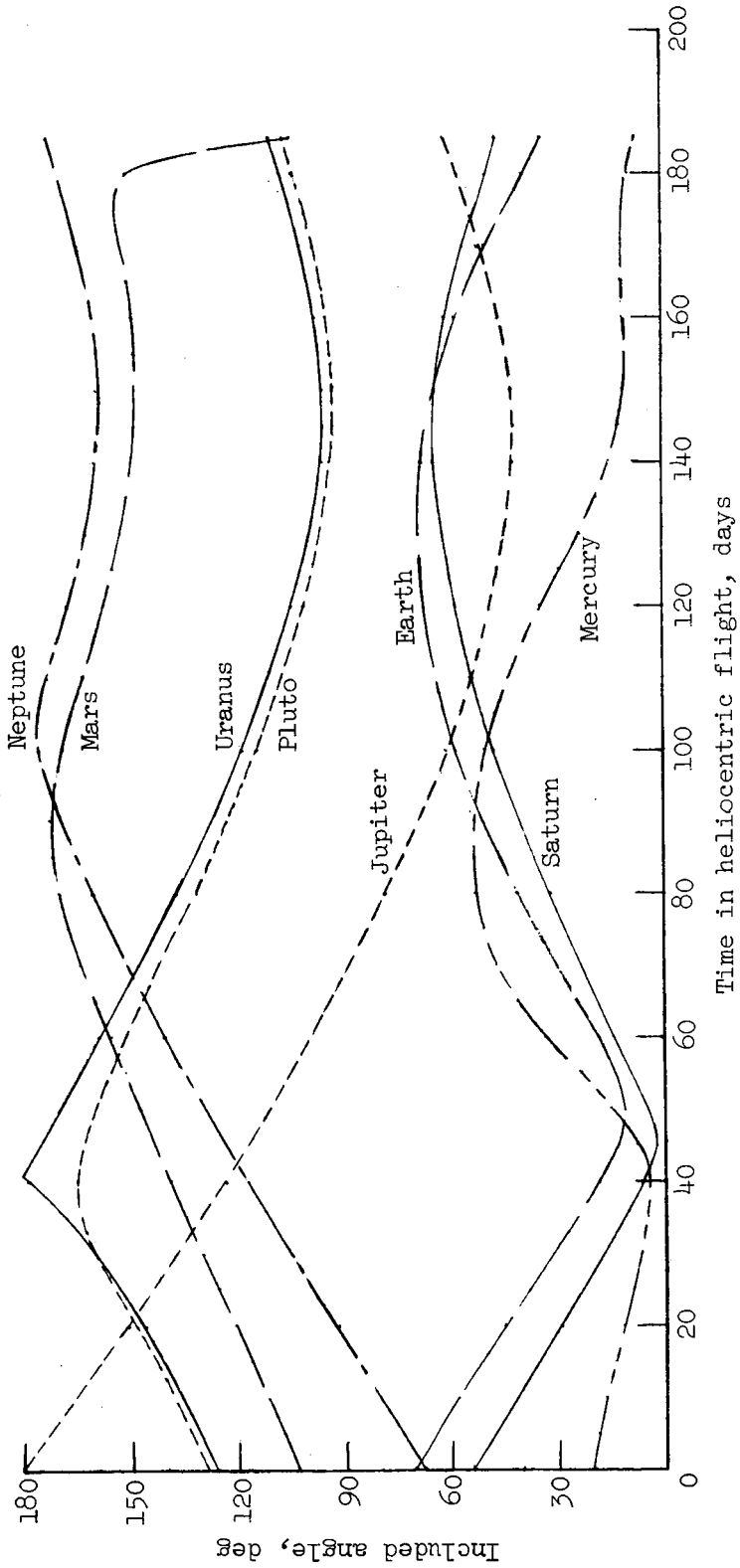


(c) Between Sun and planets.
 Figure 7.- Continued.



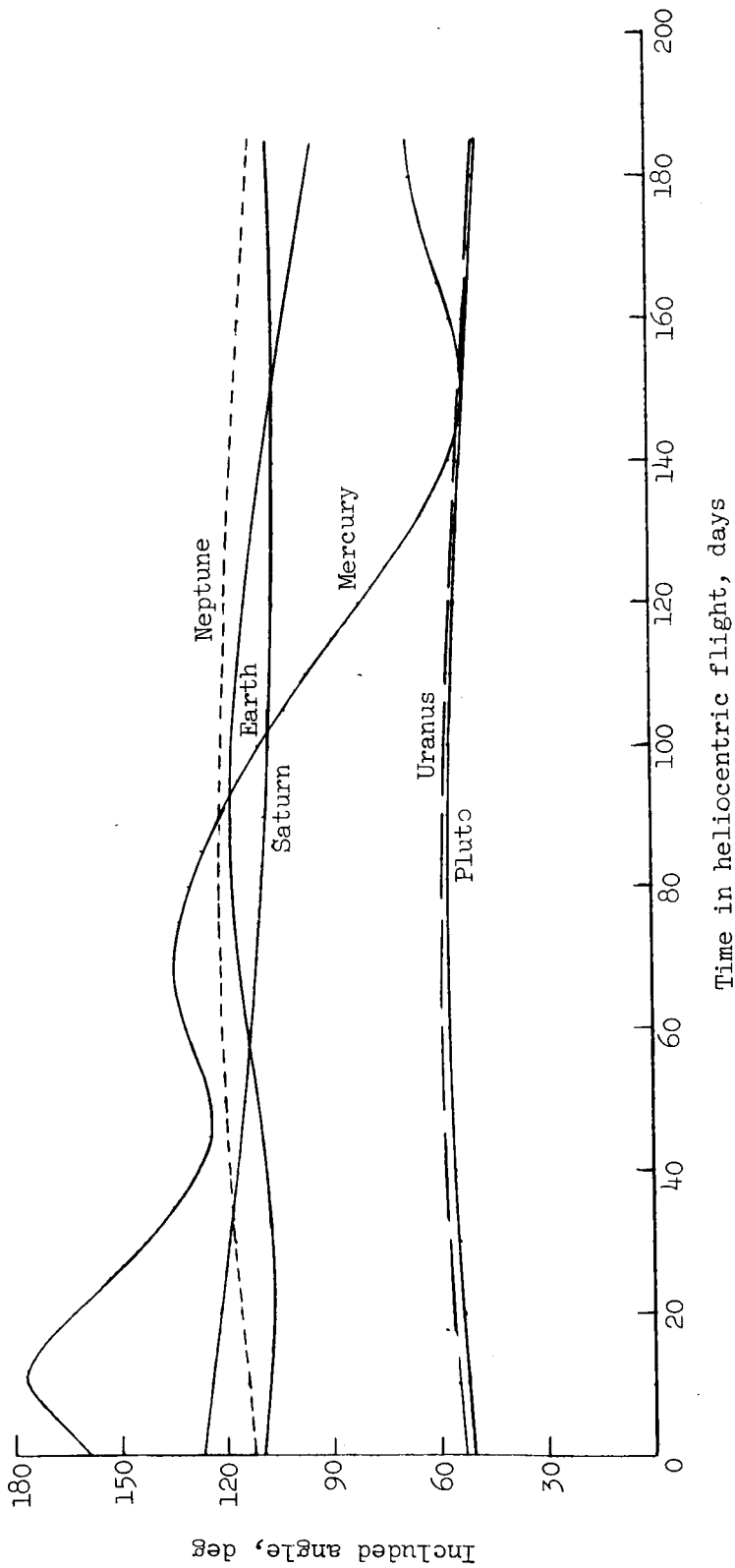
(d) Between Mars and other planets.

Figure 7.- Continued.



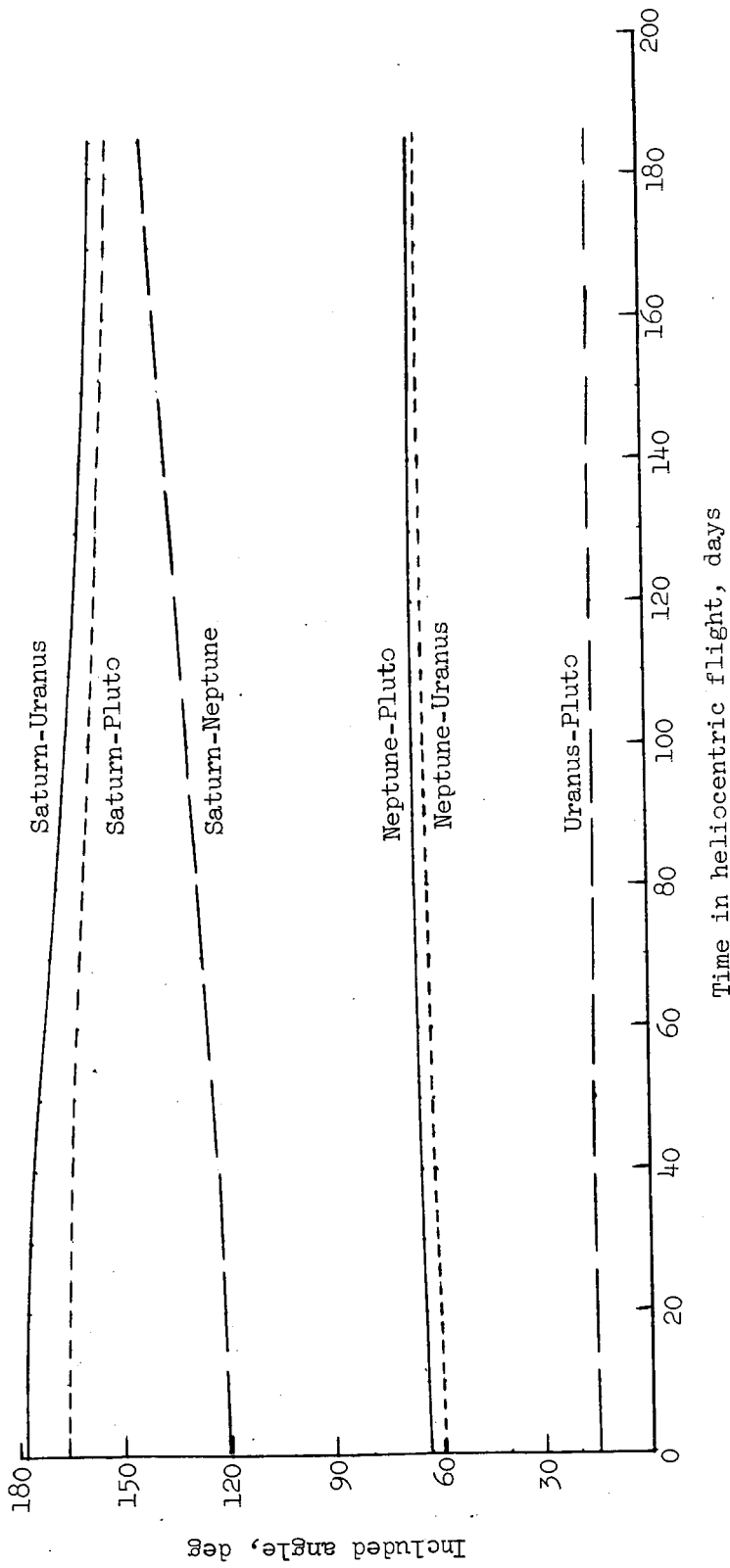
(e) Between Venus and other planets.

Figure 7.- Continued.



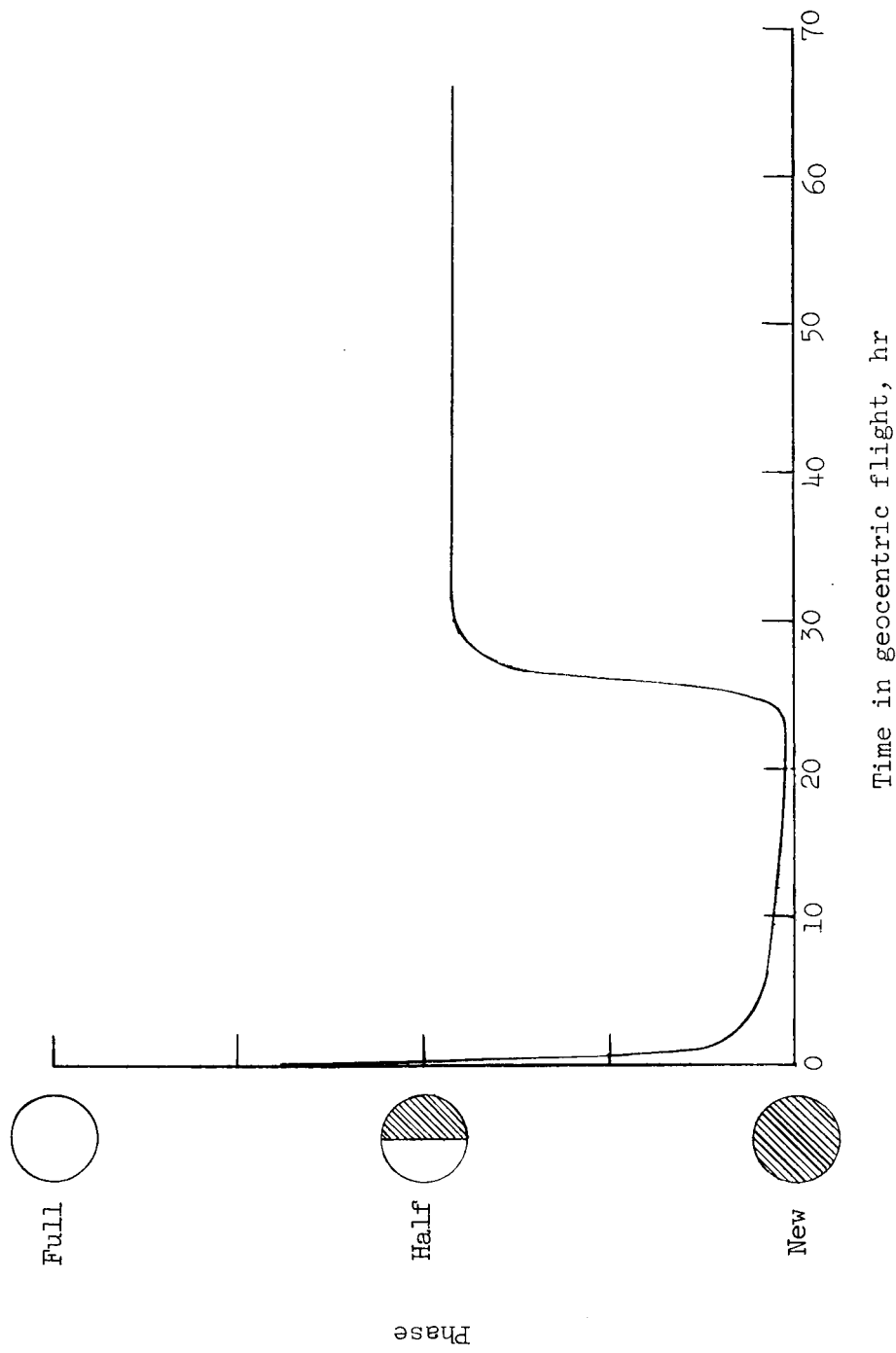
(f) Between Jupiter and other planets.

Figure 7.- Continued.



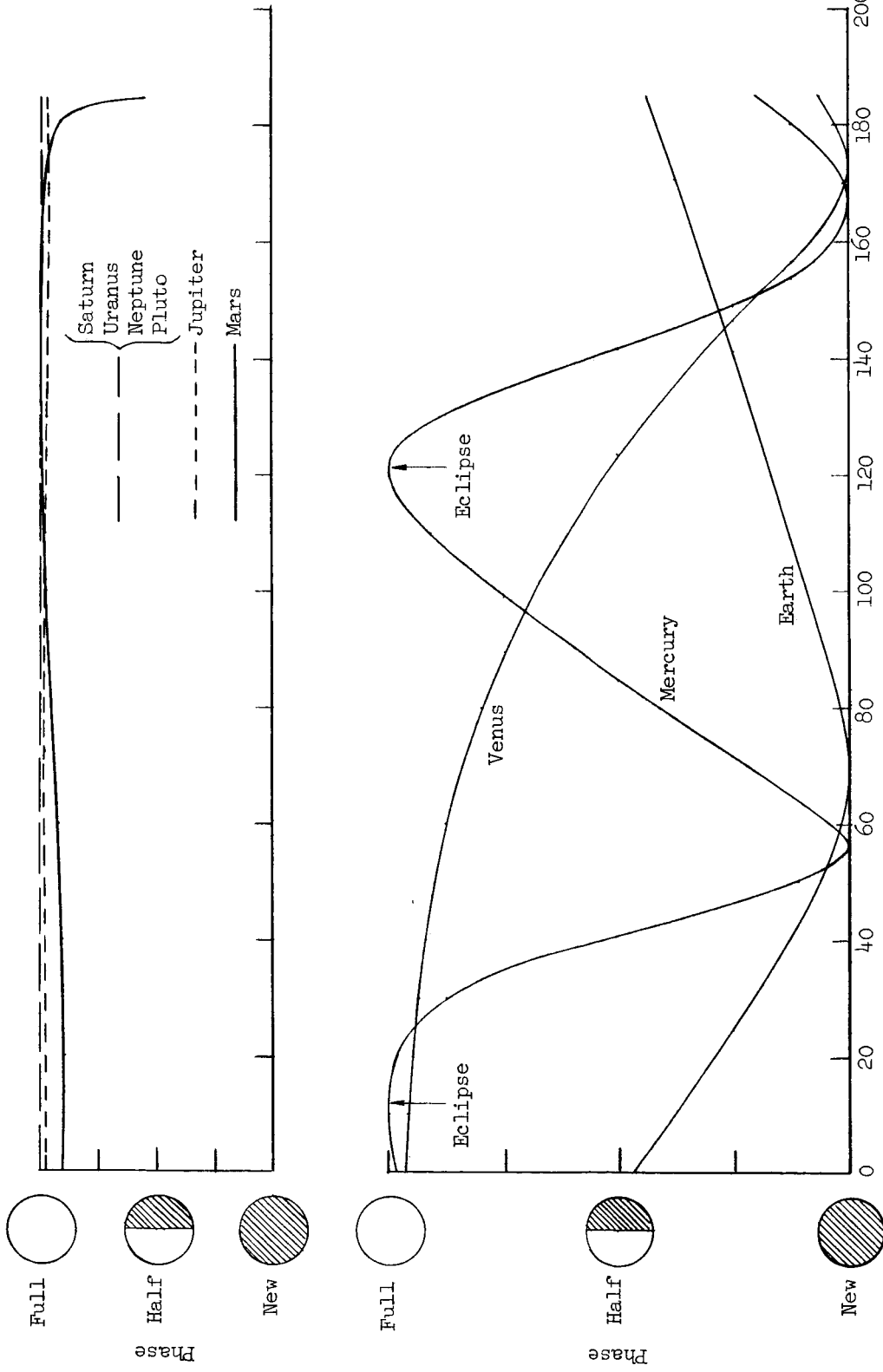
(g) Between various planets.

Figure 7.- Concluded.



(a) Phases of Earth during geocentric flight.

Figure 8.- Planetary phases as observed from spacecraft.



Time in heliocentric flight, days

(b) Phases of planets during heliocentric flight.

Figure 8.- Concluded.